JPET Fast Forward. Published on August 17, 2007 as DOI: 10.1124/jpet.107.128017

JPET #128017

Mitochondrially-targetted Effects of Berberine on K1735-M2 Mouse Melanoma Cells – Comparison with Direct Effects on Isolated Mitochondrial Fractions

Gonçalo C. Pereira, Ana F. Branco, Júlio A. C. Matos, Sandro L. Pereira, Donna Parke, Edward L. Perkins, Teresa L. Serafim, Vilma A. Sardão, Maria S. Santos, Antonio J. M. Moreno, Jon Holy and Paulo J. Oliveira*

Center for Neurosciences and Cell Biology, Department of Zoology, University of Coimbra, Portugal (GCP, AFB, JACM, SLP, TLS; VAS, MSS, PJO), Institute for Marine Research (IMAR), Department of Zoology, University of Coimbra, Portugal (AJMM), Department of Biochemistry and Molecular Biology, University of Minnesota Medical School, Duluth, USA (ELP, DP), Department of Anatomy, Microbiology and Pathology, University of Minnesota Medical School, Duluth, USA (JH)

* to whom correspondence should be addressed:

Paulo J. Oliveira, Ph.D.

Center for Neurosciences and Cell Biology, Department of Zoology, University of Coimbra, P-3004-517 Coimbra, PORTUGAL

E-mail: pauloliv@ci.uc.pt, phone: 351-239-855760, fax: 351-239-855789

Classification: Toxicology

Running title: Berberine toxicity on mitochondria

number of text pages: 43
tables: 8
figures: 11
references: 39
number of words in:
Abstract: 229
Introduction: 605
Discussion: 2416

Abbreviations List: ADP – Adenosine Diphosphate; AMP – Adenosine Monophosphate; ANT – Adenine Nucleotide Translocator; ATP – Adenosine Triphosphate; CM-H_2DCFDA – Chloromethyl Dichlorodihydrofluorescein Diacetate Acetyl Ester; CsA – Cyclosporin A; DMSO – Dimethyl Sulphoxide; EM – Electron Microscopy; FCCP – Carbonyl Cyanide p-Trifluoromethoxyphenylhydrazone; MPT – Mitochondrial Permeability Transition; mtDNA – mitochondrial DNA; RCR – Respiratory Control Ratio; ROS – Reactive Oxygen Species; RT-PCR – Real Time Polymerase Chain Reaction; SEM – Standard Error of the Mean; TMRM – Tetramethyl Rhodamine Methyl Ester; TPP^+ - Tetraphenylphosphonium cation.

Abstract

Berberine is an alkaloid present in plant extracts and has a history of use in traditional Chinese and Native American medicine. Because of its ability to arrest the cell cycle and cause apoptosis of several malignant cell lines, it has received attention as a potential anti-cancer therapeutic agent. Previous studies suggest that mitochondria may be an important target of berberine, but relatively little is known about the extent or molecular mechanisms of berberine-mitochondrial interactions. The objective of the present work was to investigate the interaction of berberine with mitochondria, both in situ and in isolated mitochondrial fractions. The data show that berberine is selectively accumulated by mitochondria, which is accompanied by arrest of proliferation, mitochondrial fragmentation and depolarization, oxidative stress and a decrease in ATP levels. Electron microscopy of berberine-treated cells shows a reduction in mitochondria-like structures, accompanied by a decrease in mtDNA copy number. Isolated mitochondrial fractions treated with berberine had slower mitochondrial respiration, especially when complex I substrates were used, and increased complex I-dependent oxidative stress. It is also demonstrated for the first time that berberine stimulates the mitochondrial permeability transition. Direct effects on ATPase activity were not detected. The present work demonstrates a number of previously unknown alterations of mitochondrial physiology induced by berberine, a potential chemotherapeutic agent, although it also suggests that high doses of berberine should not be used without a proper toxicology assessment.

Introduction

Berberine (Natural Yellow 18, 5,6-Dihydro-9,10-dimethoxybenzo(g)-1,3-benzodioxolo(5,6-a)quinolizinium, Fig. 1) is an isoquinoline alkaloid, usually extracted from rhizomes and roots from plants such as the *Berbis*, *Coptis* and *Hydrastis* species. Such herbs have long been used in traditional Chinese and Native American medicine for the treatment of several maladies. Several pharmacologic properties have been attributed to berberine, including anti-inflammatory (Kuo et al., 2004), anti-microbial (Stermitz et al., 2000), anti-diarrheal (Rabbani et al., 1987), anti-proliferative (Letasiova et al., 2006), anti-oxidative (Shirwaikar et al., 2006) and vaso-relaxant (Ko et al., 2000) actions. Different types of effects such as up-regulation of cyclooxygenase-2 (Fukuda et al., 1999) and HIF-1 (Lin et al., 2004) expression, modulation of multi-drug resistance protein (MDR) expression (Lin et al., 1999), reduction of amyloid-β peptide (Aβ) levels (Asai et al., 2007), formation of DNA adducts (Kuo et al., 1995), and cell cycle arrest (Lin et al., 2006; Mantena et al., 2006b) were also previously reported.

The anti-proliferative properties of berberine raise the interesting possibility that the compound may be useful for anti-cancer therapeutics, and berberine has been shown to promote cell death in several transformed cell lines (Hwang et al., 2006; Lee et al., 2006; Letasiova et al., 2006; Lin et al., 2006; Mantena et al., 2006b). Apoptosis induced by berberine involves activation of caspases (Hwang et al., 2006; Lin et al., 2006; Mantena et al., 2006b), increased Bax expression (Lin et al., 2006; Mantena et al., 2006b), DNA fragmentation (Kuo et al., 1995; Hwang et al., 2006; Letasiova et al., 2006; Mantena et al., 2006b) and cytochrome c release (Hwang et al., 2006; Lin et al., 2006)

suggesting a possible role of mitochondria in the process (Mantena et al., 2006a; Jantova et al., 2007) Mitochondria could be involved via release of cytochrome c, which can occur through Bax interaction with mitochondrial membranes, as well as through the formation of the mitochondrial permeability transition pore (MPT pore) (Bouchier-Hayes et al., 2005). The MPT pore can be defined as a voltage-dependent, cyclosporin A (CsA)-sensitive, high-conductance channel of the inner mitochondrial membrane. Under the experimental conditions used in most *in vitro* studies, the MPT is accompanied by mitochondrial depolarization, respiratory inhibition or stimulation, matrix swelling, matrix pyridine nucleotides (PN) depletion and release of intermembrane proteins, including cytochrome c (Bernardi et al., 2006).

Apoptosis is an active process which requires cell energy for its execution. The cellular energy pool has an important role determining if cells die by apoptosis or necrosis (Kirveliene et al., 2003). In addition, the cell cycle also requires energy. CDK–cyclin complexes ensure orderly passage through the cell cycle by the appropriate temporal phosphorylation of specific target proteins. When the cellular energy pool is lower, such target proteins are de-phosphorylated and cell cycle arrest occurs (Gemin et al., 2005). Mitochondrial generation of ATP can therefore be considered a significant control mechanism that helps govern both cell cycle progression and programmed cell death. Consequently, mitochondria hold a great promise as targets for therapeutic intervention.

For the present work, mouse melanoma K1735-M2 cells, a highly invasive melanoma cell line (Helige et al., 1993), were used to investigate berberine effects on cell proliferation and *in situ* mitochondrial physiology. In addition, isolated mitochondrial fractions were used in order to investigate direct berberine effects. We verified that berberine is accumulated by mitochondria in K1735-M2 mouse melanoma cells, causing

mitochondrial fragmentation, depolarization and oxidative stress. Results obtained in isolated mitochondrial fractions confirmed induction of oxidative stress by berberine with complex I substrates. Also, the present work describes an overall inhibition of mitochondrial respiration that appears more extensive when complex I substrates are used. It is demonstrated for the first time that berberine also enhances the calcium-induced MPT.

Materials and Methods

Materials

Berberine hemisulfate was obtained from Sigma Chemical Co. (St. Louis, Missouri, USA) and prepared in dimethyl sulphoxide (DMSO). The total volume of DMSO was always lower than 0.1 %, which had negligible effects in all experiments. Nevertheless, total volume was always lower than 0.1 %. Tetramethylrhodamine methylesther (TMRM), Hoechst 33342 and Calcein-AM were obtained from Molecular Probes (Carlsbad, California, USA). All other compounds were of the highest grade of purity commercially available.

Animals

Male Wistar rats (10 weeks old), housed at 22 ± 2ºC under artificial light for a 12-h light/day cycle and with access to water and food *ad libitum*, were used throughout the experiments. The research procedure was carried out in accordance with the European

Requirement for Vertebrate Animal Research and with the internal Standards for Animal Research at the CNC.

Cell culture

K1735-M2 mouse melanoma cells (kindly offered by Dr. Lillian Repesh, Department of Anatomy, Microbiology, and Pathology, University of Minnesota School of Medicine, Duluth, USA) were cultured in Dulbecco's modified Eagle's medium (GIBCO, Grand Island, NY) with 10% Fetal Clone III (FC3; HyClone, Logan, UT) in an atmosphere of 5% CO_2 at 37ºC.

Assessment of cell proliferation

Sulforhodamine B assays were conducted to measure the effects of berberine on the proliferation of K1735-M2 cells, as described in (Papazisis et al., 1997). Cells were seeded at a concentration of 1 x 10^4 cells/ml in 24-well plates, and allowed to recover for 1 day prior to drug addition. One of the wells was dried and washed once with PBS in order to be used as a measure of cell mass at time zero. Berberine at various concentrations (0, 10, 25, 50, 75 and 100 μM) was incubated with K1735-M2 cells for 24 h, 48 h, 72 h and 96 h, times at which the plates were collected. After cell fixation and sulforhodamine labeling, absorbance was measured in a spectrophotometer at 540 nm; the amount of dye released is proportional to the number of cells present in the dish, and is a reliable indicator of cell proliferation.

JPET Fast Forward. Published on August 17, 2007 as DOI: 10.1124/jpet.107.128017
This article has not been copyedited and formatted. The final version may differ from this version.

Confocal and epifluorescence imaging of K1735-M2 cells

Cells were seeded in glass bottom-dishes (P35G-1.5-14-C, Matek Corporation, Ashland, MA) at a concentration of 1-2 x 10^4 cells per ml. Cells were allowed to attach for 24 hours and then treated with berberine or with solvent (DMSO) for the desired time.

a) Detection of berberine mitochondrial accumulation: Berberine is a fluorescent compound, and its localization in cells was visualized using a Nikon Eclipse TE2000U epifluorescence microscope and a fluorescein filter set. Hoechst 33342 (2 µg/ml) was added to cells 30 minutes before the end of the berberine exposure time. FCCP (10 µM) was pre-incubated with one set of cells treated with berberine to investigate whether dissipation of mitochondrial membrane potential alters berberine accumulation.

b) Labelling with Hoechst 33342, TMRM and Calcein-AM: Before the ending of drug exposure time, cells in glass-bottom dishes were incubated with TMRM (100 nM), Hoechst 33342 (1 µg/ml) and calcein-AM (300 nM) for 30 minutes at 37°C in the dark. Due to the very low fluorescence of the probes in the extracellular media, the images were collected without replacing the cell culture media. The images were obtained using a Nikon C-1 laser scanning confocal microscope. TMRM signal was acquired using a green He-Ne laser. the calcein-AM signal was acquired using an air-cooled argon laser, and the Hoechst signal was obtained by using a violet diode laser. DIC images using the confocal microscope were collected using the air-cooled argon laser and the appropriate detector.

c) Quantification of TMRM mitochondrial fluorescence: Cells were seeded, treated with TMRM as described above, and visualized with a Nikon Eclipse TE2000U epifluorescence microscope. Using Metamorph software (Universal Imaging, Downingtown, PA), cells were analyzed in terms of their mean TMRM fluorescence

values and also in terms of the standard deviation (SD) values for the fluorescence of each cell. The SD values were used to characterize the effects of berberine of mitochondrial TMRM florescence as they give a more precise idea of the magnitude of the difference between cytosolic and mitochondrial TMRM accumulation.

Electron microscopy (EM) of K1735-M2 cells

After treatment, trypsinized cells were fixed for electron microscopy by adding 3% glutaraldehyde in 0.1 M sodium cacodylate buffer, pH 7.3, and were incubated for 2 h at 4°C. After centrifugation (2,500 ×g, 3 min), pellets were washed with 0.1 M sodium cacodylate buffer (pH 7.3), and resuspended in 1% OsO_4 buffered with sodium cacodylate 0.1M, pH 7.3. After 2 h incubation, pellets were washed with cacodylate buffer pH 7.3, and embedded in 1% agar. Samples were then dehydrated in ethanol and embedded in Spurr's resin. Ultrathin sections were obtained with a LKB ultra-microtome Ultrotome III and stained with methanolic uranyl acetate followed by lead citrate, and examined with a Jeol Jem-100SX electron microscope operated at 80 kV. 5-10 micrographs were taken from random fields and mitochondrial profiles observed. Each field contained 1-2 cells. By definition, mitochondrial bodies are structures which possessed morphological features of mitochondria, including a double membrane system and inner cristae.

Determination of mitochondrial DNA copy number

Total genomic nuclear and mtDNA from M2 cells was isolated using GenElute Mammalian Genomic DNA Miniprep Kit (SIGMA-Aldrich). Standard curves were generated from the control DNA sample using serial dilutions. Quantitative real-time

JPET Fast Forward. Published on August 17, 2007 as DOI: 10.1124/jpet.107.128017
This article has not been copyedited and formatted. The final version may differ from this version.

PCR using the LightCycler system (Roche Diagnostics) was performed and the following reaction components were prepared: 3.6 µl water, 0.2 µl forward primer (0.2 µM), 0.2 µl reverse primer (0.2 µM) and 5.0 µl LightCyler (Roche Diagnostics). LightCycler mixture (9 µl) was filled in the LightCycler glass capillaries and 1 µl of DNA sample (2ng) was added as PCR template. 5COI and 3COI are mtDNA primers (Thundathil et al., 2005) and MuRTGADD45a (ACCCCGATAACGTGGTACTG) and MuGADD45R (TGACCCGCAGGATGTTGATG) are Mouse GADD45 genomic DNA primers that sit in exon3. Capillaries were closed, centrifuged and placed into the LightCycler rotor. The following LightCycler experimental run protocol was used: denaturation program (95°C for 30sec), amplification and quantification program repeated 50 times (95°C for 5 s, 60°C for 20 s, 72°C for 20 s), melting curve program (95º-45º-95°C with a final heating rate of 0.1°C per second and a continuous fluorescence measurement) and finally a cooling step to 40°C. The crossing points (CP) for each transcript based on the standard curves were mathematically determined.

Determination of oxidative stress in live cells

Vital imaging of oxidative stress in K1735-M2 was determined according to the protocol described by Sardão (Sardao et al., 2007). Cells seeded in glass-bottom dishes were incubated with CM-H_2DCFDA (7.5 µM) for 1 hour at 37°C in the dark. Media was then replaced by new pre-warmed DMEM and then cells were returned to the incubator for another hour. Media was then again replaced by 2 ml of Krebs buffer (1 mM $CaCl_2$, 132 mM NaCl, 4 mM KCl, 1.2 mM Na_2HPO_4, 1.4 mM $MgCl_2$, 6 mM Glucose, 10 mM HEPES, pH 7.4). Cells were observed by epifluorescence microscopy using a Nikon Eclipse

TE2000U microscope (fluorescein filter) and images were obtained using Metamorph software (Universal Imaging, Downington, PA).

Adenine nucleotide extraction from cells in culture

An acid extraction procedure was used to evaluate the intracellular concentration of adenine nucleotides. Both adherent and non-adherent (dead) cells were collected. Adenine nucleotides were separated by reverse-phase high performance liquid chromatography. The chromatographic apparatus was a Beckman-System Gold, consisting of a 126 Binary Pump Model and a 166 Variable UV detector, computer-controlled. The detection wavelength was 254 nm, and the column was a Lichrospher 100RP-18 (5 µm) from Merck (Dramstadt, Germany). An isocratic elution with 100 mM phosphate buffer (KH_2PO_4), pH 6.5 and methanol 1% was performed with a flow rate of 1.1 mL/minutes. The required time for each analysis was 5 minutes. Quantification was achieved by employing ATP, ADP and AMP standard curves.

Isolation of rat liver mitochondria

Mitochondria were isolated from liver of male Wistar rats by conventional methods with slight modifications. Homogenization medium contained 250 mM sucrose, 10 mM HEPES (pH 7.4), 1 mM EGTA, and 0.1% fat-free BSA. EGTA and BSA were omitted from the final washing medium, adjusted at pH 7.2. The mitochondrial pellet was washed twice, suspended in the washing medium, and immediately used. Protein content was determined by the biuret method (Gornall et al., 1949) calibrated with bovine serum albumin (BSA).

Oxygen consumption

Oxygen consumption of isolated liver mitochondria was polarographically monitored with a Clark oxygen electrode connected to a suitable recorder in a 1 mL thermostated, water-jacketed, closed chamber with magnetic stirring at a constant temperature of 30 ºC. The standard respiratory medium consisted of 135 mM sucrose, 65 mM KCl, 2.5 mM $MgCl_2$, 5 mM KH_2PO_4, 5 mM HEPES (pH 7.2). Mitochondria were suspended at a concentration of 1.5 mg/mL in the respiratory medium. Respiration was started by adding 5 mM glutamate plus malate or 5 mM succinate with 3 µM rotenone. ADP (125 nmol) was added to initiate state 3 respiration. Oligomycin (1 µg) and FCCP (1 µM) were also added to the system in order to inhibit passive proton flux through the ATP synthase and to uncouple respiration, respectively. Berberine was pre-incubated with mitochondria in the reaction medium for 2 minutes before the addition of the respiratory substrate.

Mitochondrial transmembrane potential

The mitochondrial transmembrane potential ($\Delta\Psi$) was indirectly estimated by the mitochondrial accumulation of the lipophilic cation tetraphenylphosphonium (TPP^+) as detected by using a TPP^+-selective electrode in combination with an Ag/AgCl-saturated reference electrode. Both the TPP^+ electrode and the reference electrode were inserted into an open vessel with magnetic stirring and were connected to a pH meter (Jenway, Model 3305). The signals were fed to a potentiometric recorder (Kipp & Zonen, Model BD 121). No correction was made for the ‘‘passive’’ binding of TPP^+ to the mitochondrial membranes, since the purpose of the experiments was to show relative changes in potentials rather than absolute values. Mitochondrial protein (1.5 mg) was suspended

under constant stirring in 1 mL of reaction medium composed of 125 mM sucrose, 65 mM KCl, 5 mM KH_2PO_4, 2.5 mM $MgCl_2$ and 5 mM Hepes (pH 7.4, 30ºC), supplemented with 3 µM TPP^+. Mitochondria were energized with 10 mM glutamate/malate or 10 mM succinate plus 3 µM rotenone. Berberine was added prior to mitochondrial protein. ADP (125 nmol) was added to initiate phosphorylation. Absolute values for membrane potential (in millivolts) were determined from the equation originally proposed by Kamo (Kamo et al., 1979), assuming Nernst distribution of the ion across the membrane electrode. A matrix volume of 1.1 µl/mg protein was assumed.

Mitochondrial Swelling

Mitochondrial osmotic volume changes were followed by the decrease of absorbance at 540 nm with a Jasco V-560 spectrophotometer. The assays were performed in 2 mL of the reaction media (200 mM sucrose, 10 mM Tris-MOPS (pH 7.4), 10 µM EGTA, 1 mM KH_2PO_4, 1.5 µM rotenone, and 2.5 mM succinate), 1,5 mg protein with constant stirring, at 30ºC. Calcium (20 µM) was added to the preparation 1 minute after to the start of the experiment. Cyclosporin A (1 µM) was added to the mitochondrial preparation before the addition of calcium to inhibit the mitochondrial permeability transition. Berberine was pre-incubated with the mitochondrial preparation for 2 min.

Mitochondrial calcium loading

Extramitochondrial free Ca^{2+} was assayed by using the hexapotassium salt of the fluorescence probe Calcium Green 5-N (100 nM) (Rajdev and Reynolds, 1993). Briefly, heart mitochondria (0.4 mg) were suspended in 2 ml of buffer containing 200 mM sucrose, 10 mM TRIS, 10 µM EGTA (to complex basal calcium), 1 mM KH_2PO_4, 2 µM

rotenone, and 4 mM succinate. Fluorescence was continuously recorded in a water-jacketed cuvette holder at 30 ºC using a Perkin-Elmer LS-55 fluorescence spectrometer with excitation and emission wavelengths of 506 and 531 nm, respectively. Slits used were 5 nm for both excitation and emission wavelengths.

Measurements of Mitochondrial Reactive Oxygen Species (ROS) Production

Intramitochondrial oxidative stress was assessed by using the probe CM-H_2DCFDA. Isolated mitochondria were incubated with CM-H_2DCFDA (4 nmol/mg protein) for 30 min under constant circular motion. Mitochondria were then centrifuged (8000xg at 4 ºC), and suspended in 1mL of a ice-cold isolation medium containing 250 mM sucrose and 10 mM Hepes-KOH (pH 7.4). Subsequently, mitochondria (1mg) were suspended in standard reaction media, supplemented with glutamate/malate (2 mM) and with the different berberine concentrations tested. Rotenone (1.5 µM) and succinate (2.5 mM) were added during different time points. DCF fluorescence was continuously recorded in a water-jacketed cuvette holder at 30 ºC using a Perkin-Elmer LS-50B fluorescence spectrometer with excitation and emission wavelengths of 485 and 520 nm (5 nm slits), respectively.

Mitochondrial ATPase activity

The effect of Berberine on mitochondrial ATPase was observed by two distinct methods: First, the activity of mitochondrial ATPase was evaluated thorough detection of pH changes occurring during ATP hydrolysis, as previously described (Carvalho et al., 1974). Mitochondria (1.5 mg protein) were incubated in 1 ml reaction media (135 mM sucrose, 65mM KCL, 2.5 mM $MgCl_2$, 5 mM KH_2PO_4) pH 7.2. Reaction was initiated by

the addition of 3 mM ATP. Oligomycin was used as a selective inhibitor of ATPase (F_o unit), and completely abolished pH alterations. Known concentrations of KOH were used to calibrate the system.

ATPase activity was also measured by the ATP-induced generation of transmembrane potential ($\Delta\psi$) by using a TPP^+-selective electrode. Mitochondria (1.5 mg protein) were incubated in 1 mL of reaction media (125 mM sucrose, 65 mM KCL, 2.5 mM $MgCl_2$, 5 mM KH_2PO_4, 5 mM HEPES) pH 7.4 at 30 ºC. The media was supplemented with 3 µM TPP^+ and 3 µM rotenone. Reaction was started by 3 µM ATP. Oligomycin was used as a selective inhibitor of ATP synthase (F_o unit).

Statistical Analysis

Data is expressed as means ± SEM and evaluated by one-way ANOVA followed by Bonferroni multiple comparison tests. Differences were considered significant if the P value was lower than 0.05.

JPET Fast Forward. Published on August 17, 2007 as DOI: 10.1124/jpet.107.128017
This article has not been copyedited and formatted. The final version may differ from this version.

Results

Effect of berberine in K1735-M2 cell line proliferation

To investigate whether berberine inhibits cell proliferation K1735-M2 mouse melanoma cells were incubated in the absence and presence of increasing concentrations of drug (5, 10, 25, 75, 100 μM) for 24, 48, 72 and 96 hours. As shown in Fig. 2, berberine has a dose-time-dependent effect inhibiting cell proliferation. Within 24h of drug treatment, cell proliferation does not seem to be affected. However, after 48h of incubation time, the growth profile changes and an inhibitory effect is observed for all drug concentrations tested. Approximately 50% of growth inhibition is observed for 72h and 96h of drug exposure. Berberine effect on cell proliferation is more dependent on time exposure than on the drug concentration because for 96h of drug exposure the majority of drug concentrations inhibit cell proliferation. As described elsewhere, the present technique cannot conclude if the effect of berberine is due to an increase of cell death or due to cell cycle arrest.

Berberine accumulates in K1735-M2 cells mitochondria

To evaluate the intracellular location of berberine accumulation, K1735-M2 cells were incubated with one selected berberine concentration (25 μM) during 6 hours and then examined by epifluorescence microscopy. In panel A of Fig. 3, clusters of green fluorescence in the cell cytoplasm are observed demonstrating intracellular berberine accumulation. A magnification of some of the cells (panel C and F) shows that the clusters resemble mitochondria. To confirm berberine localization, an indirect method

using FCCP, a mitochondrial uncoupler, was chosen, since co-localization with other mitochondrial probes (*viz.* TMRM or Mitotracker Red) interfered with berberine localization and self-fluorescence (data not shown). When FCCP was used to dissipate the mitochondrial the mitochondrial electric potential, the results demonstrated that no mitochondrial berberine accumulation could be detected in the presence of FCCP (panel D). The observation confirms that berberine is accumulated electrophoretically, i.e., with a dependence on the mitochondrial transmembrane electric potential. Interestingly, when mitochondrial membrane potential was collapsed with FCCP, nuclear berberine fluorescence occurs (panel E), which suggests that in the absence of an electric gradient, berberine can be accumulated in the nuclei.

Berberine causes mitochondrial damage on K1735-M2 melanoma cells

To investigate alterations of mitochondrial morphology induced by berberine, cells were treated with berberine (5 – 50 μM) for 6 and 24 hours (Fig. 4). 45 minutes before the end of the incubation period, cells were incubated with TMRM. Larger concentrations were not tested due to the strong interference of berberine self-fluorescence. It was observable that alterations in mitochondrial membrane potential (decreased mitochondrial TMRM signal) and morphology (mitochondrial fragmentation) are already observed for 6 hours (25 and 50 μM). For 24 hours, the effects are greatly enhanced and alterations appear already for 10 μM berberine. Measurements up to 96 hours were already performed using the same protocol. For such long time-points, a complete dissipation of TMRM signal was observed in most cells (data not show). Only a few cells

JPET Fast Forward. Published on August 17, 2007 as DOI: 10.1124/jpet.107.128017
This article has not been copyedited and formatted. The final version may differ from this version.

showed small round (instead of filamentous) mitochondria still retaining TMRM (data not show).

To explore in detail mitochondrial alterations caused by berberine, we mostly focused in one berberine concentration (25 μM) as the objective was to cause notorious mitochondrial damage with concentrations not lacking relevance in *in vivo* systems. Cells incubated with berberine were fluorescently labelled with Hoechst 33342 and TMRM. Mitochondrial accumulation of TMRM results in red fluorescence. As berberine also presents red fluorescence, a conflict between both signals could be a problem. However, TMRM has a higher fluorescence quantum yield so the contribution of berberine fluorescence is non-significant. Panel A and B of Fig. 5 shows that after 24 hours of treatment, the filamentous mitochondrial network is dismantled and mitochondria appear to be smaller and rounder in shape. Alterations in mitochondrial structure occur with intact cell viability, as observed by intracellular calcein-AM accumulation and TMRM fluorescence (panel C). Mitochondrial fragmentation did not increase the apparent number of mitochondrial bodies as observed by EM. In fact, by visualizing several fields from each treatment group, a lower number of mitochondrial bodies was observed after berberine treatment, although determination of mitochondrial mass by EM warrants several notes of caution. By comparing the two panels (A and B) of Fig. 5 it is also observable that loss of mitochondrial TMRM fluorescence accompanies fragmentation even for 6 hours of exposure (panel I and J). 50 μM berberine was used in order to investigate if a dose-dependent effect could be found. In fact, the depolarization effect obtained with the higher concentration was not dissimilar from the result obtained with the lower concentration. The panel F of Fig. 5 shows

control condensed mitochondria where cristae can be easily observed. In contrast, most mitochondrial bodies lost their typical shape, swelled and appear to loose their cristae after a 24h incubation period with berberine, although different degrees of damage were observable (panel D-H, Fig. 5). The apparent decrease in mitochondrial numbers by electron microscopy was also supported by the finding that mtDNA copy number decreases when cells are treated with 25 µM of berberine for 24h and 48h (Fig. 5K). Surprisingly, when that maximum berberine concentration used in proliferation studies (100 µM) was used, no decrease in mtDNA copy number occurred.

The normal processes that occur in an apoptotic cell such as nucleus/chromatin condensation, membrane blebbing and the formation of apoptotic bodies, was not observed at the concentrations of berberine used in this study (up to 100 µM; data not shown).

Berberine increases intracellular oxidative stress

To test whether berberine increases oxidative stress, cells were incubated with the drug (25 µM) for 6 and 24 hours. 45 minutes before the end of incubation period, cells were incubated with Hoechst 33342, TMRM and CM-H_2DCFDA, a fluorescent probe for oxidative stress. Fig. 6 shows that 6 hours of exposure is not enough to cause a significant increase in intracellular oxidative stress as opposed to 24 hours of drug exposure when an increase of probe fluorescence was observed in cells treated with 25 µM berberine. We also confirmed that the mitochondrial depolarization precedes the detection of oxidative stress.

Berberine decreases energy charge in K1735-M2 cells

Berberine decreases cellular energy charge (([ATP] + 0.5 [ADP]) / ([ATP] + [ADP] + [AMP])), with the greatest decreases occurring after 72 hours (Table 1). The ratio of ATP/ADP was also altered by berberine when cells were incubated for 24 hours (Table 1). Interestingly, for longer exposure periods the effects of berberine on the ATP/ADP ratio is decreased. In fact, for 72 hours the ratio is not dissimilar from the control. Regarding the specific type of adenine nucleotide affected by berberine, the results (Table 2) demonstrate that ATP quantity decreases within 24 hours in the presence of 25 μM berberine. As opposed to the unchanged ATP/ADP ratio found for 72 hours, there is a statistically significant change in ATP concentration between control and treated cells. The unchanged ratio described in Table 1 is caused by the simultaneous decrease of ADP, which is also accompanied by increased AMP levels. The overall results indicate that both ATP and ADP are decreased by berberine treatment, while AMP concentrations increase. FCCP, a mitochondrial uncoupler, shows similar results to that of berberine suggesting a possible equivalence of targets and mechanisms of action. None of the drugs or concentrations tested altered the total number of adenine nucleotides.

Berberine affects mitochondrial oxygen consumption

The effect of berberine on mitochondrial oxygen consumption with both glutamate/malate and succinate as substrates is described in Tables 3 and 4 respectively. Under the range of concentration up to 66.7 nmol berberine/mg protein berberine decreases the respiratory control ratio (RCR) for both respiratory substrates (absolute values of control 6.0±0.67 for glutamate/malate and 4.1±0.43 for succinate).

However, the decrease is more evident when the substrate for complex I is used (approximately 80% vs. 50% when succinate is used at the highest berberine concentration). The ADP/O ratio remained unchanged for both types of substrate except for the higher concentrations (33.35 and 66.7 nmol berb/mg protein) where a significant decrease can be observed (absolute values of control 2.2 ± 0.21 for glutamate/malate and 1.6 ± 0.15 for succinate). The results suggest an effect on the electron transfer chain (predominantly at the complex I level) but also a possible interference in the mitochondrial phosphorylation system. The values for the RCR of the control group denote a good mitochondrial preparation, which is further confirmed by the ADP/O values. In the presence of the uncoupler FCCP, respiration is progressively decreased by berberine regardless of the drug concentration or respiratory substrate. However, it must be stressed that mitochondrial respiratory state 3 is more strongly inhibited compared to uncoupled respiration when mitochondria are energized by complex I substrates as observed in Figure 7 (panel A). When liver mitochondria were energized with a complex II substrate, respiratory state 3 decreased in a similar fashion to uncoupled respiration. When glutamate/malate is used, mitochondrial respiratory state 4 is not altered except for the highest berberine concentration used (100 μM). When mitochondria are energized by succinate an increase of oxygen consumption in mitochondrial respiratory state 4 is observed instead but this effect is abolished when oligomycin is added suggesting a possible increased passive flux of protons through the F_O subunit of the ATP synthase. Stimulation of respiration during state 4 is not observed when mitochondria are energized by glutamate/malate, as more severe inhibition of the respiratory chain may hide the effect.

Berberine affects the generation of mitochondrial membrane potential

When analyzing the effects of berberine on mitochondrial ΔΨ generation (Table 5 and 6 and Fig. 8), only the highest concentrations have significant effects on the maximal ΔΨ generated. The differences are more drastic when parameters related with the phosphorylation system are analyzed, namely the depolarization induced by ADP and the phosphorylation lag phase. The effects are observable for both substrates. It should be noted that for higher drug concentrations, mitochondria do not recover their normal ΔΨ values after ADP addition. The results again suggest that the effects of berberine on isolated mitochondrial fractions are most evident when mitochondria are challenged to increase their respiration rate, either by using ADP or FCCP.

Berberine stimulates the MPT on isolated rat liver mitochondria

One of the effects of MPT pore opening is mitochondrial swelling due to osmotic equilibrium between the matrix and the external compartment, leading to water influx. The effect of berberine on Ca^{2+} / Pi-induced mitochondrial swelling was studied by measuring the changes in the suspension absorbance at 540 nm, in a sucrose-based media. Figure 9 shows that berberine in a range up to 133.2 nmol/mg protein increases swelling of isolated liver mitochondria in the presence of 20 μM of calcium. Surprisingly, the mitochondrial swelling rate augmented by berberine does not appear to be dose dependent because at higher concentrations, swelling slows without a decrease in amplitude (Table 7). These results were confirmed by oxygen consumption when calcium was added to mitochondria energized with succinate (data not shown)., The MPT pore inhibitor Cyclosporin A (CsA) (Broekemeier et al., 1989) was able to prevent

mitochondrial swelling in the presence of berberine, confirming that this effect is caused by the induction of the MPT pore.

Berberine decreases mitochondrial calcium loading capacity

In order to confirm that berberine induces MPT pore opening, we evaluated mitochondrial calcium loading capacity in the presence of this alkaloid. Extramitochondrial calcium levels were followed by using the fluorescence probe Calcium Green 5N. Shortly after an increase in probe fluorescence due to calcium addition, fluorescence decreased in all conditions tested, indicating mitochondrial calcium uptake. However, berberine, in a dose-dependent fashion (Fig. 10, lines 1-3), decreased calcium accumulation when compared with controls. When mitochondria were pre-incubated with CsA, calcium-induced calcium release in the presence of berberine was inhibited. The data confirms that berberine decreases mitochondrial calcium loading capacity through increased MPT pore induction.

Berberine increases ROS production on isolated mitochondria

In order to determine if the increase in oxidative stress observed in berberine-treated cells also occurs in isolated mitochondrial fractions, intramitochondrial oxidative stress was measured using the fluorescent probe CM-H_2DCFDA. To pinpoint a possible source of increased oxidative stress in the respiratory chain, we used different substrates and a specific complex I inhibitor (rotenone, 1.5 µM). As demonstrated in Fig. 11 there were no significant differences when compared with the control except for the lowest berberine concentration (6.7nmol/mg). When using glutamate-malate as substrate and in the absence of rotenone, probe oxidation was higher in the presence of 6.7 nmol berberine /

mg protein when compared with the control. The fluorescence of the probe (due to oxidation) decreased when rotenone was added to the system. No differences were observed when succinate in the presence of rotenone was used, regardless of the berberine concentration used. The observation leads us to assume that ROS production can be localized downstream to the rotenone binding site on complex I.

Berberine does not affect ATPase activity

The differences observed in the ADP/O parameter, along with berberine-induced differences in ADP depolarization and phosphorylation lag phase as obtained by using a TPP^+ selective electrode, suggested that this alkaloid may have a negative effect on mitochondrial ATP synthase (complex V). In order to test this possibility, ATPase activity experiments were performed. By using two distinct methods no statistically significant differences were observed between control and berberine-treated mitochondria (Table 8), indicating that berberine apparently does not inhibit complex V activity.

Discussion

Medicinal herbs have been used for millennia to treat or prevent several maladies such as cancer (Dorai and Aggarwal, 2004). Since most active compounds responsible for the pharmacological effect are still unknown, the literature is rich in research involving purification of the active components and evaluation of their pharmacological use. An important aspect is to investigate the toxic effects of phytochemicals found in traditional

medicine on biological systems, as many formulations may be found in over-the-counter medications.

In the present work we demonstrate that berberine inhibits the proliferation of K1375-M2 mouse melanoma cells. Although we did not specifically measure the contributions of cell death and/or cell cycle arrest, it appears that concentrations of berberine up to 100 μM do not cause significant levels of death in these cells. By morphological analysis, no typical alterations characteristic of apoptosis or necrosis were found (Serafim et al., 2007). Therefore, the inhibition of proliferation (Fig. 2) results from cell cycle arrest instead of cell death. Our data contrasts with works from other laboratories (Kuo et al., 1995; Hwang et al., 2006; Letasiova et al., 2006; Lin et al., 2006; Mantena et al., 2006b), where berberine was found to promote apoptosis. However, many of these studies used concentrations of berberine much higher than those used here. Also, different cell lines have been show to exhibit significantly different sensitivities to apoptotic induction by berberine (Letasiova et al., 2006).

The advantages of the fluorescence properties of berberine were used to demonstrate that the drug primarily accumulates in mitochondria. These results are in agreement with previous studies (Serafim et al., 2007) where we demonstrated that berberine is accumulated primarily in mitochondria at lower concentrations (up to about 50 μM) but becomes detectable in the nucleus and cytoplasm at higher concentrations (over 50 μM), possibly due to saturation of the mitochondrial compartment. Berberine is a positively charged isoquinolinium molecule; such compounds are more active inhibitors of the mitochondrial respiratory chain than uncharged molecules when tested on isolated mitochondria (Barreto et al., 2003), which may reflect a stronger affinity for the

JPET Fast Forward. Published on August 17, 2007 as DOI: 10.1124/jpet.107.128017
This article has not been copyedited and formatted. The final version may differ from this version.

negatively charged matrix. Likewise, we demonstrate that the mitochondrial electric transmembrane potential is a driving force for drug accumulation, as FCCP prevents mitochondrial berberine fluorescence. Mikes and Dadak (1983) presented similar results although an increase in berberine fluorescence quantum yield upon mitochondrial energization was suggested as the explanation (Mikes and Dadak, 1983). One crucial piece of data from our results is the appearance of berberine fluorescence in nuclei or cytoplasm after incubation of cells with FCCP and berberine concentrations that do not normally stain nuclei and cytoplasm. One would expect that if mitochondrial-localized berberine was mostly losing its fluorescence quantum yield upon FCCP treatment, then nuclei and cytoplasm should not change their fluorescence characteristics. The primary accumulation in mitochondria vs. other cell compartments can also help explain the effect of the compound in promoting cell cycle arrest vs. cell death. In fact, certain other positively charged isoquinolines are primarily accumulated in the nucleus and act through promoting cell death (e.g., sanguinarine, Matos *et al.*, in preparation) with few alterations in mitochondrial bioenergetics (Barreto et al., 2003).

Mitochondria are well known to produce free radicals as a consequence of mitochondrial respiration (Sastre et al., 2000). Assays with dichlorofluorescein, a probe whose fluorescence increase in the presence of oxidants, show that berberine increases oxidative stress in K1735-M2 cells. In order to clarify if increased oxidative stress results from mitochondrial interactions, experiments on isolated mitochondria were conducted. Results show that berberine, for the lowest concentration tested, increases oxidative stress on isolated liver mitochondria when using complex I substrates, which may help explain results in intact cells exposed to berberine. Increased oxidative stress can be attributed to an interaction of berberine at a site downstream of the rotenone binding site

as this inhibitor inhibits berberine-induced oxidative stress. Even without using alternative inhibitors of the respiratory chain, it is likely that the site is located on complex I as berberine does not produce significant oxidative stress in rotenone-treated mitochondria energized with succinate. These actions resemble those of doxorubicin, an anthracycline used in anti-cancer therapy that generates oxidative stress at mitochondrial complex I (Berthiaume and Wallace, 2007). As described, increased oxidative stress occurs only for the lowest berberine concentrations, which can explained by a report demonstrating that berberine possesses antioxidant properties (Hwang et al., 2002). It is possible that at lower concentrations, pro-oxidant actions through inhibition of Complex I outweigh the antioxidant activity of berberine, whereas at higher concentrations, the anti-oxidant activity prevails over the pro-oxidant effects.

It is reasonable to think that berberine, once accumulated within the mitochondria, affects oxidative phosphorylation efficiency and compromises the normal behaviour of the cell. The decrease in cell ATP concentration observed after berberine treatment can explain the cell cycle arrest as ATP has been described to regulate the cell cycle (Gemin et al., 2005).

When comparing standard respiratory parameters in isolated rat liver mitochondria, berberine inhibition of oxygen consumption is more pronounced when respiratory substrates for complex I are used. Barreto et. al. (2003) have also demonstrated that berberine affects more the activity of the isolated NADH dehydrogenase (complex I) when compared with the isolated succinate dehydrogenase (complex II). Mikes et al. (Mikes and Dadak, 1983; Mikes and Yaguzhinskij, 1985) also observed that berberine derivatives have a predominant effect on mitochondrial complex I. The results from the present study indicate that although berberine appears to have a predominant effect

when complex I substrates are used, succinate-sustained respiration is also inhibited, suggesting a broader range of targets in the respiratory chain.

The analysis of ADP/O, ADP depolarization and lag phase also suggest that berberine interacts with the mitochondrial phosphorylative system. One of the constituents of the phosphorylative system is the ATP synthase which is responsible for the production of ATP. Two distinct experiments show that berberine does not affect complex V activity. However there are others constituents of the phosphorylative system such as the adenine nucleotide transporter (ANT) or the phosphate uniporter that can also be possible targets for berberine action. In fact, one attractive candidate is the ANT, as it is also a component of the MPT pore (see below). Work is currently underway to clarify this question. The effects of berberine on isolated mitochondria can explain the decrease in energy status observed in intact cells treated with this alkaloid.

The presence of berberine in mitochondria seems to increase the susceptibility to MPT pore opening since swelling amplitude is increased when berberine is added. Results obtained using a fluorescent calcium probe confirmed the swelling results, indicating that berberine decreases mitochondrial calcium loading capacity through increased induction of the MPT pore. Interestingly, electron microscopy shows that most mitochondria from berberine-treated cells are swollen, pale, and lack identifiable cristae, suggesting that they have undergone the MPT. MPT pore opening in intact cells is still a controversial topic as several cytosolic factors may alter MPT pore gating properties. However, the occurrence of the MPT pore induced by berberine is a possible explanation to the decreased number of mitochondrial bodies and swollen aspect of most mitochondria.

Although normal liver and cancer cell mitochondria may present certain structural and functional differences, we believe that sufficient similarities exist to justify using isolated

liver mitochondria as models to gain insights into the actions of xenobiotic compounds with the mitochondrial system of malignant cells. Also, isolated fractions present the advantage of a much higher isolation yield so that more aspects of mitochondrial function can be studied with one single isolation procedure.

Two observations from this work deserve future attention. First, we have observed that berberine enhances the calcium-induced permeability transition in isolated liver mitochondrial fractions, and at least from morphological data, apparently as well in intact cells. We tried to use cyclosporin A to test the possibility that berberine also stimulates the MPT in intact cells but berberine effects were actually exacerbated (data not shown), which can be attributed to inhibition of berberine efflux by cyclosporin A (Sonneveld and Wiemer, 1997). It is interesting that the enhanced MPT occurrence in intact cells, if confirmed, did not result in K1735-M2 cell death, although it is reasonable to speculate that the decrease in mitochondrial mass may be related with mitochondrial destruction induced by the MPT. The second interesting observation deals with the decrease of mtDNA copy number for 25 µM but not for 100 µM. Berberine is known to intercalate into double-stranded DNA, forming adducts that can inhibit DNA replication (Kuo et al., 1995), which could explain the reduced mtDNA copy numbers in cells treated with low concentrations of berberine. It is possible that the lack of reduction in mtDNA copy number in cells treated with 100 µM berberine reflects a compensatory mechanism that attempts to overcome the decreased mitochondrial ATP production by increased mtDNA copy number. Alternatively, it could be that the higher levels of oxidative stress induced by lower concentrations of berberine result in mtDNA destruction that is either blocked by the anti-oxidant effects of higher concentrations of berberine, or somehow inhibited by a “protective” effect of a larger quantity of intercalated berberine. It would be of

interest to obtain and compare accurate measures of mitochondrial mass with mtDNA quantity in cells treated with different concentrations of berberine.

During several cell events (including apoptosis) mitochondrial fragmentation is observed which results in smaller, rounder and more numerous mitochondria (Arnoult, 2007). The results from epifluorescence microscopy show that the mitochondrial network is dissipated after berberine treatment but the number of mitochondria does not increase as shown by EM. A possible explanation is that the fragmented mitochondria are damaged and end up being destroyed. The results demonstrate that mitochondrial network is strongly affected by berberine but the cause is not immediately clear. It has been demonstrated that oxidative stress causes mitochondrial fragmentation (Sardao et al., 2007) and the increased oxidative stress observed after treatment with low doses of berberine could explain the vesiculation of the mitochondrial network observed by epifluorescence microscopy. Unfortunately, the extensive mitochondrial depolarization induced by high concentrations of berberine makes observation of mitochondrial morphology with charge-dependent probes like TMRM difficult.

The present work shows that berberine is accumulated by mitochondria of a mouse melanoma cell line, leading to mitochondrial fragmentation and dysfunction, accompanied by decreased cellular energy charge. When the effect was compared with the results obtained on isolated mitochondrial fractions, it is observed that regardless of the system used, berberine is toxic for mitochondria. One major limitation of the present study (as in many others) is the lack of knowledge of the real concentration of berberine that reaches mitochondria in intact cells. Although we do not possess data regarding this aspect, it is wise to speculate that mitochondrial berberine concentrations will be much higher than in the bulk cytosol due to electrophoretic accumulation. We believe that the

range of berberine concentrations accumulated by mitochondria in intact cells is within the range of concentrations used on isolated mitochondrial fractions in the present study.

The present work not only provides insights on the mechanism by which berberine interferes with tumor cell proliferation, demonstrating previously unknown effects on mitochondrial physiology but also raises a note of caution on the use of berberine as a non-toxic “natural” over-the-counter medication.

References

Arnoult D (2007) Mitochondrial fragmentation in apoptosis. *Trends Cell Biol* **17**:6-12.

Asai M, Iwata N, Yoshikawa A, Aizaki Y, Ishiura S, Saido TC and Maruyama K (2007) Berberine alters the processing of Alzheimer's amyloid precursor protein to decrease A beta secretion. *Biochem Biophys Res Commun* **352**:498-502.

Barreto MC, Pinto RE, Arrabaca JD and Pavao ML (2003) Inhibition of mouse liver respiration by Chelidonium majus isoquinoline alkaloids. *Toxicol Lett* **146**:37-47.

Bernardi P, Krauskopf A, Basso E, Petronilli V, Blalchy-Dyson E, Di Lisa F and Forte MA (2006) The mitochondrial permeability transition from in vitro artifact to disease target. *Febs J* **273**:2077-2099.

Berthiaume JM and Wallace KB (2007) Adriamycin-induced oxidative mitochondrial cardiotoxicity. *Cell Biol Tox* **23**:15-25.

Bouchier-Hayes L, Lartigue L and Newmeyer DD (2005) Mitochondria: pharmacological manipulation of cell death. *J. Clin Invest* **115**:2640-2647.

Broekemeier KM, Dempsey ME and Pfeiffer DR (1989) Cyclosporine-a Is a Potent Inhibitor of the Inner Membrane-Permeability Transition in Liver-Mitochondria. *J Biol Chem* **264**:7826-7830.

Carvalho AP, Vale MG and Madeira VM (1974) Regulation of Atpase of Sarcoplasmic-Reticulum (Sr) Studied in Presence of Antibiotic X-537a. *Fed Proc* **33**:1332-1332.

Dorai T and Aggarwal BB (2004) Role of chemopreventive agents in cancer therapy. *Cancer Lett* **215**:129-140.

Fukuda K, Hibiya Y, Mutoh M, Koshiji M, Akao S and Fujiwara H (1999) Inhibition by berberine of cyclooxygenase-2 transcriptional activity in human colon cancer cells. *J Ethnopharmacol* **66**:227-233.

Gemin A, Sweet S, Preston TJ and Singh G (2005) Regulation of the cell cycle in response to inhibition of mitochondrial generated energy. *Biochem Biophys Res Communs* **332**:1122-1132.

Gornall AG, Bardawill CJ and David MM (1949) Determination of serum proteins by means of the biuret reaction. *J Biol Chem* **177**:751-766.

Helige C, Smolle J, Zellnig G, Finkpuches R, Kerl H and Tritthart HA (1993) Effect of Desqualinium on K1735-M2 Melanoma Cell-Growth, Directional Migration and Invasion Invitro. *Europ J Cancer* **29A**:124-128.

Hwang JM, Kuo HC, Tseng TH, Liu JY and Chu CY (2006) Berberine induces apoptosis through a mitochondria/caspases pathway in human hepatoma cells. *Arch Toxicol* **80**:62-73.

Hwang JM, Wang CJ, Chou FP, Tseng TH, Hsieh YS, Lin WL and Chu CY (2002) Inhibitory effect of berberine on tert-butyl hydroperoxide-induced oxidative damage in rat liver. *Arch Toxicol* **76**:664-670.

Jantova S, Cipak L and Letasiova S (2007) Berberine induces apoptosis through a mitochondrial/caspase pathway in human promonocytic U937 cells. *Toxicol in Vitro* **21**:25-31.

Kamo N, Kobatake Y, Muratsugu M and Hongoh R (1979) Membrane potential of mitochondria measured with an electrode sensitive to tetraphenyl phosphonium and relationship between proton electrochemical potential and phosphorylation potential in steady state. *J Membr Biol* **49**:105-121.

Kirveliene V, Sadauskaite A, Kadziauskas J, Sasnauskiene S and Juodka B (2003) Correlation of death modes of photosensitized cells with intracellular ATP concentration. *FEBS Lett* **553**:167-172.

Ko WH, Yao XQ, Lau CW, Law WI, Chen ZY, Kwok W, Ho K and Huang Y (2000) Vasorelaxant and antiproliferative effects of berberine. *Eur J Pharmacol* **399**:187-196.

Kuo CL, Chi CW and Liu TY (2004) The anti-inflammatory potential of berberine in vitro and in vivo. *Cancer Lett* **203**:127-137.

Kuo CL, Chou CC and Yung BYM (1995) Berberine Complexes with DNA in the Berberine-Induced Apoptosis in Human Leukemic Hl-60 Cells. *Cancer Lett***93**:193-200.

Lee HJ, Son DH, Lee SK, Lee J, Jun CD, Jeon BH, Lee SK and Kim EC (2006) Extract of Coptidis rhizoma induces cytochrome-c dependent apoptosis in immortalized and malignant human oral keratinocytes. *Phyto Res* **20**:773-779.

Letasiova S, Jantova S, Cipak L and Muckova M (2006) Berberine - antiproliferative activity in vitro and induction of apoptosis/necrosis of the U937 and B16 cells. *Cancer Lett* **239**:254-262.

Lin HL, Liu TY, Wu CW and Chi CW (1999) Berberine modulates expression of mdr1 gene product and the responses of digestive track cancer cells to Paclitaxel. *Br J Cancer* **81**:416.

Lin JP, Yang JS, Lee JH, Hsieh WT and Chung JG (2006) Berberine induces cell cycle arrest and apoptosis in human gastric carcinoma SNU-5 cell line. *World J Gastroenter* **12**:21-28.

Lin SK, Tsai SC, Lee CC, Wang BW, Liou JY and Shyu KG (2004) Berberine inhibits HIF-1 alpha expression via enhanced proteolysis. *Mol Pharm* **66**:612-619.

Mantena SK, Sharma SD and Katiyar SK (2006a) Berberine inhibits growth, induces G(1) arrest and apoptosis in human epidermoid carcinoma A431 cells by regulating Cdki-Cdk-cyclin cascade, disruption of mitochondrial membrane potential and cleavage of caspase 3 and PARP. *Carcinogenesis* **27**:2018-2027.

Mantena SK, Sharma SD and Katiyar SK (2006b) Berberine, a natural product, induces G(1)-phase cell cycle arrest and caspase-3-dependent apoptosis in human prostate carcinoma cells. *Mol Cancer Therap* **5**:296-308.

Mikes V and Dadak V (1983) Berberine Derivatives as Cationic Fluorescent-Probes for the Investigation of the Energized State of Mitochondria. *Biochim Biophys Acta* **723**:231-239.

Mikes V and Yaguzhinskij LS (1985) Interaction of Fluorescent Berberine Alkyl Derivatives with Respiratory-Chain of Rat-Liver Mitochondria. *J Bioenerg Biomemb* **17**:23-32.

Papazisis KT, Geromichalos GD, Dimitriadis KA and Kortsaris AH (1997) Optimization of the sulforhodamine B colorimetric assay. *J Immunol Meth* **208**:151-158.

Rabbani GH, Butler T, Knight J, Sanyal SC and Alam K (1987) Randomized Controlled Trial of Berberine Sulfate Therapy for Diarrhea Due to Enterotoxigenic Escherichia-Coli and Vibrio-Cholerae. *J Infect Dis* **155**:979-984.

Rajdev S and Reynolds IJ (1993) Calcium Green-5N, a Novel Fluorescent-Probe for Monitoring High Intracellular Free Ca^{2+} Concentrations Associated with Glutamate Excitotoxicity in Cultured Rat-Brain Neurons. *Neurosc Lett* **162**:149-152.

Sardao VA, Oliveira PJ, Holy J, Oliveira CR and Wallace KB (2007) Vital imaging of H9c2 myoblasts exposed to tert-butylhydroperoxide - characterization of morphological features of cell death. *BMC Cell Biol* **8**.

Sastre J, Pallardo FV and Vina J (2000) Mitochondrial oxidative stress plays a key role in aging and apoptosis. *IUBMB Life* **49**:427-435.

Serafim TL, Oliveira PJ, Sardao VA, Perkins E, Parke D, Holy J (2007), Different concentrations of berberine result in distinct cellular localization patterns and cell cycle effects in a melanoma cell line. *Cancer Chemother Pharmacol.* (*in press)*

Shirwaikar A, Shirwaikar A, Rajendran K and Punitha ISR (2006) In vitro antioxidant studies on the benzyl tetra isoquinoline alkaloid berberine. *Biol Pharm Bull* **29**:1906-1910.

Sonneveld P and Wiemer E (1997) Inhibitors of multidrug resistance. *Curr Opin Oncol* **9**:543-548.

Stermitz FR, Lorenz P, Tawara JN, Zenewicz LA and Lewis K (2000) Synergy in a medicinal plant: Antimicrobial action of berberine potentiated by 5 '-methoxyhydnocarpin, a multidrug pump inhibitor. *Proc Natl Acad Sci USA* **97**:1433-1437.

Thundathil J, Filion F and Smith LC (2005) Molecular control of mitochondrial function in preimplantation mouse embryos. *Mol Reprod Dev* **71**:405-413.

Legends for Figures

Figure 1 - Chemical structure of berberine (5,6-Dihydro-9,10-dimethoxybenzo(g)-1,3-benzodioxolo(5,6-a)quinolizinium)).

Figure 2 – Anti-proliferative effect of berberine in K1735-M2 mouse melanoma cell proliferation profile. Cells (1.0×10^5) were incubated and drugged 24h later with a range of concentrations up to 100 µM during 24, 48, 72 and 96 hours. Cell proliferation was accessed at each time by the SRB colorimetric assay as described in Materials and Methods and plotted against time of exposure and concentration of berberine. Data presented as means ± SEM of four different experiments.

Figure 3 - Berberine accumulation in mitochondria of K1735 -M2 mouse melanoma cells after 6 hours of drug exposure evaluated by epifuorescence microscopy. Berberine presents green fluorescence which allows identifying the intracellular site of drug accumulation. A) Accumulation of 25 µM berberine in control cells (berberine self-fluorescence). B) Hoechst 33342 labeling of field shown in A. C) Magnification of some of the cells in panel A. D) No berberine signal is observable when cells were pre-incubated with 10 µM FCCP, a mitochondrial uncoupler. E) Hoechst 33342 labeling of field shown in D. F) Magnification of some cells shown in panel D. Cells were observed with an epifluorescence microscope by using the FITC filter. Nuclei were labeled with Hoechst 33342. Bar represents 30 µm.

Figure 4 – Dose-dependent effects of berberine on mitochondrial TMRM accumulation and overall morphology. Cells were incubated with crescent concentrations (numbers at the left, in μM) of berberine for 6 and 24 hours. 45 minutes before the end of the incubation time, cells were incubated with the mitochondrial fluorimetric probe TMRM, which accumulates according to the mitochondrial electric membrane potential. The most noticeable alterations which appear dependent on the incubation time and berberine concentration are loss of mitochondrial TMRM accumulation (reflecting mitochondrial depolarization) and breakage of mitochondrial filamentous. White bar denotes 15 μm.

Figure 5 - Mitochondrial alterations induced by berberine. The effects of berberine on mitochondrial structure were evaluated by using confocal and electron microscopy. MtDNA copy numbers were evaluated by using RT-PCR.

Panels A and B: Confocal microscopy of K1735-M2 cells treated with vehicle (A) and 25 μM berberine (B) during 24 hours. White bar denotes 15 μm. Live cells were labelled with the fluorescent probes TMRM (mitochondria) and Hoechst 33342 (nuclei) for 30 minutes before observation with a confocal microscope. *Panel C* shows a detail of a cell treated with 25 μM berberine during 24 hours, where fragmented and round mitochondria labelled with TMRM can be observed. Hoechst 33342 (nucleus) and calcein-AM (cytoplasm) were the two other probes used. Cytoplasmic calcein granules are also observable although their origin is yet to identify. *Panels D and E*: Electron microscopy (white bars represent 5 μm) showing K1735-M2 cells treated with vehicle (D) and 25 μM berberine (E) during 24 hours. The white arrow indicates mitochondrial

bodies. Panels F, G and H: Electron microscopy showing K1735-M2 cells treated with vehicle (F), 10 µM (G) and 25 µM berberine (H) during 24 hours. The white arrow indicates mitochondrial bodies. All three panels are the same magnification. Panels I and J: Evaluation of TMRM fluorescence in cells treated with vehicle, 25 µM and 50 µM berberine for 6 (I) and 24 (J) hours. Quantification of cell fluorescence was made as described in the materials and methods section. * $p < 0.05$ vs control. Panel K: MtDNA copy number of cells treated with vehicle, 25 or 100 µM berberine. Relative mtDNA copy numbers were determined as described in the materials and methods section.

Figure 6 - Berberine induced mitochondrial depolarization and increased oxidative stress in K1735-M2 mouse melanoma cells. Cells were incubated with 25 µM berberine for 6 or 24 hours. 45 minutes before the end of the incubation period, the fluorescent probes TMRM (red, mitochondria), Hoechst 33342 (blue, nuclei) and CM-H_2DCFDA (green, oxidative stress) were incubated with cells and imaged with a Nikon Eclipse 3000 epifluorescence microscope.

Figure 7 - Typical recording of the effect of berberine on mitochondrial oxygen consumption. Mitochondria (1.5 mg) were incubated in 1 ml of standard reaction media as described in Material and Methods. Respiration was started by adding 5 mM glutamate plus malate (*Panel A*) or 5 mM succinate with 3 µM rotenone (*Panel B*). ADP (125 nmol) was added to initiate state 3. Oligomycin (1 µg) and FCCP (1 µM) were also added to the system in order to inhibit passive flux through the ATP synthase and to uncouple respiration, respectively. Berberine 6.67 nmol/mg (2), 16.68 (3), 33.35 (4), 66.7 (5) was pre-incubated during 2 minutes. Line 1 corresponds to the control situation.

Figure 8 - Representative recording of mitochondrial electric potential measured with a TPP^+ -selective electrode. Rat liver mitochondria (1.5mg) were incubated in 1 ml of the medium supplemented with 3 µM TPP^+. Energization of the mitochondrial population was achieved with 10 mM glutamate-malate (*Panel A*) or 10 mM succinate plus 3 µM rotenone (*Panel B*). After stabilization of the recording, 125 nmol ADP was added. For more details see Materials and Methods section. Line 2 corresponds to the lowest berberine concentration tested (6.67 nmol / mg protein) and line 3 corresponds to the highest concentration tested (66.7 nmol / mg protein). Line 1 corresponds to the control situation.

Figure 9 - Typical recording of the effect of berberine on Ca^{2+} / Pi-induced mitochondrial swelling evaluated by the decrease of optical density at 540 nm caused by calcium. Mitochondria (1.5 mg) were energized by succinate. After a basal line was established, 20 µM calcium was added to induce the MPT pore. Berberine was incubated with mitochondria in the following amounts (in nmol/mg protein): 13.3 (3); 33.3 (4); 66.6 (5); 100.0 (6); 133.2 (7). Line 2 corresponds to the control situation. Cyclosporin A was pre-incubated before the addition of calcium and was able to prevent mitochondrial swelling (1). The recordings showed here are representative of at least four different separated mitochondrial preparations.

Figure 10 - Assessment of mitochondrial calcium loading capacity in the presence of berberine. Berberine was incubated with mitochondria (0.4 mg) in the following amounts:

1 - 31.2 nmol/mg, 2 - 15.6 nmol/mg, 3 - 6.2 nmol/mg, 5 - 31.2 nmol/mg of berberine in the presence of Cyclosporin A (100nM). Line 4 corresponds to the control situation. The fluorescent probe Calcium Green 5-N (100nM) was used to evaluate the levels of extramitochondrial calcium as described in Materials and Methods.

Figure 11 - Evaluation of intramitochondrial ROS production by using the fluorescent probe CM-H_2DCFDA. Mitochondria (1 mg) were incubated in 2 ml of the standard reaction media (250 mM sucrose and 10 mM Hepes-KOH, pH 7.4) as described in the Materials and Methods section. After pre-determined time intervals, rotenone (1.5 μM) and succinate (2.5 mM) were added to the system. The graphic shows the variation of fluorescence rate relative to the control condition. White bars – Glutamate/Malate, Gray bars – Glutamate/Malate in the presence of rotenone, Black bars – Succinate. * $p < 0.05$ vs. respective control.

Tables

Table 1 - Effects of berberine in the energy charge and ATP/ADP ratio in K1735-M2 mouse melanoma cells. FCCP, a mitochondrial uncoupler, was added as a positive control. Energy charge was calculated as ([ATP] + 0.5 [ADP]) / ([ATP] + [ADP] + [AMP]). Data are means ± SEM of at least 4 different preparations. * $p < 0.05$ vs control for each time of incubation.

			Berberine				FCCP
		CTL	10 µM	25 µM	50 µM	100 µM	10 µM
Energy Charge	24 h	0.41 ± 0.03	0.33 ± 0.03	0.30 ± 0.03	0.27 * ± 0.05	0.23 * ± 0.04	0.25 * ± 0.03
	48 h	0.50 ± 0.04	0.40 ± 0.04	0.33 * ± 0.03	0.27 * ± 0.04	0.25 * ± 0.04	0.28 * ± 0.03
	72 h	0.52 ± 0.06	0.27 * ± 0.04	0.23 * ± 0.03	0.22 * ± 0.04	0.25 * ± 0.03	0.30 * ± 0.04
ATP / ADP	24 h	1.43 ± 0.26	0.88 * ± 0.13	0.76 * ± 0.10	0.63 * ± 0.04	0.64 * ± 0.07	0.80 * ± 0.06
	48 h	1.50 ± 0.15	1.28 ± 0.11	1.11 ± 0.12	0.96 * ± 0.04	0.93 * ± 0.13	1.18 ± 0.10
	72 h	1.58 ± 0.18	1.41 ± 0.14	0.98 ± 0.13	1.27 ± 0.28	1.16 ± 0.15	1.03 ± 0.22

Table 2 - Effects of berberine on adenine nucleotides levels of K1735-M2 mouse melanoma cells. Cells ($1.0x10^5$) were treated with berberine in a range up to 100 µM at different incubation times. FCCP, a mitochondrial uncoupler, was added as a positive control. Adenine nucleotides quantification was realized as described in Material and Methods and data is described as percentage of total nucleotides. Data are means ± SEM of at least 4 different preparations. * $p < 0.05$ vs control for each incubation time.

			Berberine				FCCP
		CTL	10 µM	25 µM	50 µM	100 µM	10 µM
Total Nucleotides (ρmol / mg protein)	24 h	1343.8 ± 268.1	1731.4 ± 207.1	2001.1 ± 249.6	2184.0 ± 377.1	1834.9 ± 460.1	2059.3 ± 225.7
	48 h	1813.4 ± 131.7	2369.6 ± 212.2	1730.0 ± 277.6	1828.4 ± 454.3	151.47 ± 140.7	1640.4 ± 273.3
	72 h	1275.2 ± 312.1	1838.1 ± 466.5	1469.6 ± 433.0	1539.1 ± 469.2	2127.4 ± 393.6	1632.3 ± 250
ATP (%)	24 h	30.2 ± 2.8	20.8 ± 3.1	18.2 * ± 2.8	15.3 * ± 3.1	13.8 * ± 2.1	15.8 * ± 2.4
	48 h	38.3 ± 3.8	28.0 ± 3.6	21.5 * ± 3.3	17.2 * ± 2.7	15.8 * ± 3.4	18.8 * ± 2.6
	72 h	39.0 ± 5.6	20.0 * ± 3.0	18.74 * ± 3.4	18.2 * ± 3.9	18.3 * ± 3.4	20.1 * ± 3.4
ADP (%)	24 h	25.0 ± 2.9	24.1 ± 1.3	23.9 ± 1.5	23.7 ± 3.3	21.3 ± 3.2	19.3 ± 1.7
	48 H	26.9 ± 1.3	24.6 ± 1.5	22.3 ± 2.2	20.3 ± 2.5	18.2 * ± 1.6	18.1 * ± 2.1
	72 H	25.2 ± 2.5	14.5 * ± 2.5	9.1 * ± 2.4	8.4 * ± 1.6	12.6 * ± 1.5	20.8 ± 2.5
AMP (%)	24 h	47.5 ± 3.7	55.0 ± 3.3	57.9 ± 3.8	61.0 ± 6.4	67.9 * ± 5.4	65.0 ± 4.0
	48 h	36.8 ± 3.7	47.4 ± 4.0	56.2 * ± 4.5	62.4 * ± 4.7	65.9 * ± 4.6	63.2 * ± 4.0
	72 h	43.0 ± 1.68	65.5 * ± 5.3	73.6 * ± 3.4	73.4 * ± 3.7	69.2 * ± 3.1	59.1 ± 5.0

Table 3 - Effects of berberine on mitochondrial respiratory parameters energized by glutamate/malate. Data represents percentage control. Mitochondria (1.5 mg) were incubated in 1 ml respiration media (see Materials and Methods) at 30 ºC. State 4 was measured in the presence of 5 mM glutamate plus malate. ADP (125 nmol) was added to induce state 3 respiration. Oligomycin (1 µg) and FCCP (1 µM) were also added to the system in order to inhibit passive flux through the ATP synthase and to uncouple respiration. The RCR was calculated as the ratio between state 3 and state 4 respiration. The ADP/O was calculated as the number of nmol ADP phosphorylated by natom oxygen consumed during ADP phosphorylation. Data are means ± SEM of 4-5 different preparations. * $p < 0.05$ vs. control. Control absolute values are expressed as natoms O/min/mg protein. Other values are expressed as % control values; n. m. = not measurable.

Berberine	CTL	6.7 nmol / mg protein	16.7 nmol / mg protein	33.4 nmol / mg protein	66.7 nmol / mg protein
State 3	59.3 ± 3.8	83.2 % ± 3.0	57.8 % ± 6.6 *	33.4 % ± 4.8 *	14.7 % ± 4.7 *
State 4	12.8 ± 0.6	107.0 % ± 9.0	99.0 % ± 13.7	105.3 % ± 14.6	47.6 % ± 7.5 *
RCR	6.0 ± 2.1	76.3 % ± 6.3 *	66.0 % ± 7.2 *	30.0 % ± 6.2 *	22.9 % ± 5.9 *
ADP/O	2.2 ± 0.7	96.4 % ± 9.2	93.3 % ± 3.3	n.m.	n. m.
Oligomycin	7.4 ± 3.0	111.6 % ± 9.3	78.5 % ± 16.2	79.2 % ± 13.7	65.3 % ± 5.8
FCCP	68.2 ± 6.7	83.8 % ± 4.1	73.9 % ± 5.2 *	61.8 % ± 6.49 *	56.4 % ± 11.4 *

Table 4 - Effects of berberine on mitochondrial respiratory parameters energized by succinate. Data represents percentage against control. Experiences were carried out in the same conditions as describe in Table 3 but with mitochondria energized with 5 mM succinate in the presence of 3 μM rotenone. Data are means ± SEM of 4-5 different preparations. * $p < 0.05$ vs. control. Control absolute values are expressed as natoms O/min/mg. protein. Other values are expressed as % control values.

Berberine	CTL	6.7 nmol / mg protein	16.7 nmol / mg protein	33.4 nmol / mg protein	66.7 nmol / mg protein
State 3	90.7 ± 10.2	90.8 % ± 5.6	75.8 % ± 1.8 *	74.6 % ± 3.6 *	58.6 % ± 4.7 *
State 4	22.6 ± 1.6	96.4 % ± 5.7	110.8 % ± 8.1	127.7 % ± 3.2 *	143.0 % ± 8.8 *
RCR	4.1 ± 0.4	93.8 % ± 4.1	69.1 % ± 4.4 *	62.4 % ± 7.0 *	44.9 % ± 4.9 *
ADP/O	1.6 ± 0.2	91.8 % ± 3.0	94.1 % ± 3.0	83.5 % ± 1.3 *	81.4 % ± 3.2 *
Oligomycin	16.4 ± 2.1	94.5 % ± 3.5	105.9 % ± 4.7	113.8 % ± 6.2	108.9 % ± 9.4
FCCP	152.7 ± 16.2	85.8 % ± 4.1	79.7 % ± 3.9 *	70.6 % ± 7.2 *	52.0 % ± 4.4 *

Table 5 - Effects of berberine on glutamate/malate-energized mitochondria. $\Delta\Psi$ max., ADP depolarization and lag phase was measured by using a TPP^+ selective electrode (see materials and methods section for further details of the method). The values present are mean ± SEM. * $p < 0.05$ vs. control. n. m. = not measurable

Berberine	$\Delta\Psi$ max. (-mV)	ADP depolarization (-mV)	Lag Phase (sec)
Control	215.2 ± 5.4 (100 %)	27.5 ± 1.8 (100 %)	24.0 ± 2.1 (100 %)
6.7 nmol / mg protein	216.5 ± 2.9 (100.9 % ± 2.6)	28.4 ± 1.5 (105.6 % ± 9.4)	30.5 ± 4.8 (124.1 % ± 9.6)
16.7 nmol / mg protein	217.7 ± 3.6 (101.4 % ± 2.6)	26.5 ± 1.6 * (98.6 % ± 8.9)	35.8 ± 5.9 (144.6 % ± 12.1)
33.4 nmol / mg protein	215.9 ± 4.9 (100.7 % ± 17.0)	24.5 ± 1.6 * (76.2 % ± 16.5)	47.1 ± 8.6 * (171.0 % ± 40.8)
66.7 nmol / mg protein	212.7 ± 5.2 * (99.1 % ± 2.9)	34.6 ± 5.7 (131.6 % ± 21.5)	n. m.

Table 6 - Effects of berberine on succinate-energized mitochondria. ΔΨ max, ADP depolarization and lag phase was measured by using a TPP^+ selective electrode (see Materials and Methods). The values presented represent means ± SEM. * $p < 0.05$ vs. control.

Berberine	ΔΨ max. (-mV)	ADP depolarization (-mV)	Lag Phase (sec)
Control	214.3 ± 5.8 (100 %)	33.5 ± 2.5 (100 %)	21.2 ±1.4 (100%)
6.7 nmol / mg protein	214.0 ± 3.2 (99.8 % ± 2.9)	28.4 ± 1.0 * (88.0 % ± 9.6)	25.8 ± 1.9 (122.9 % ± 10.2)
16.7 nmol / mg protein	212.7 ± 3.5 (99.6 % ± 3.0)	24.1 ± 1.3 ***** (74.8% ± 8.9)	29.2 ± 2.7 (139.5 % ± 13.9)
33.4 nmol / mg protein	209.9 ± 4.0 * (98.2 % ± 3.1)	17.9 ± 1.7 ***** (55.8 % ± 8.2)	37.2 ± 4.1 ***** (178.1 % ± 21.0)
66.7 nmol / mg protein	206.2 ± 4.1 ***** (96.5 % ± 3.0)	11.3 ± 2.0 ***** (35.6 % ± 7.1)	45.6 ± 3.0 ***** (179.2 % ± 37.1)

Table 7 - Effects of different berberine concentrations (numbers in the left column) on Ca^{2+} / Pi-induced mitochondrial swelling parameters studied by measuring absorbance changes in the suspension in a sucrose-based media. Swelling amplitude was calculated as the difference between basal line absorbance and the absorbance after 500 sec. Rate values represent the initial mitochondrial swelling rate after the addition of calcium. Data are means ± SEM of at least four different experiments. * $p < 0.05$ vs control; $^{\#}$ $p < 0.05$ vs Ca^{2+} + 133.2 nmol berberine / mg protein.

	Amplitude (A.U.)	Swelling Rate (A.U. / min)
Ca^{2+} alone	- 0.465 ± 0.182	- 0.045 ± 0.041
Ca^{2+}+13.3 nmol/mg protein	- 1.147 ± 0.084 *	- 0.277 ± 0.041
Ca^{2+}+33.3 nmol/mg protein	- 1.198 ± 0.059 *	- 0.505 ± 0.065 *
Ca^{2+}+66.6 nmol/mg protein	- 1.295 ± 0.050 *	- 0.472 ± 0.100 *
Ca^{2+}+100 nmol/mg protein	- 1.045 ± 0.237 *	- 0.367 ± 0.142 *
Ca^{2+}+133.2 nmol/mg protein	- 1.281 ± 0.119 *	- 0.346 ± 0.035
Ca^{2+}+133.2 nmol/mg protein + CsA	- 0.241 ± 0.159 $^{\#}$	- 0.047 ± 0.036 $^{\#}$

JPET Fast Forward. Published on August 17, 2007 as DOI: 10.1124/jpet.107.128017
This article has not been copyedited and formatted. The final version may differ from this version.

Table 8 - Measurement of ATPase activity using two distinct methods: in the first column, the detection of pH changes associated with ATP hydrolysis was measured with a pH electrode (see Materials and Methods); in the second method tested. Δψ generated by ATP hydrolysis was measured by using a TPP-selective electrode. Values are means ± SEM of 3 different mitochondrial preparations. * $p < 0.05$ vs control.

	nmol H^+ / mg protein	Δψ (-mV)
Control	3.6 ± 0.2	166.8 ± 2.0
33.4 nmol berberine / mg protein	3.9 ± 0.2	166.6 ± 1.6
66.7 nmol berberine / mg protein	4.1 ± 0.4	167.7 ± 1.4

FIG.1

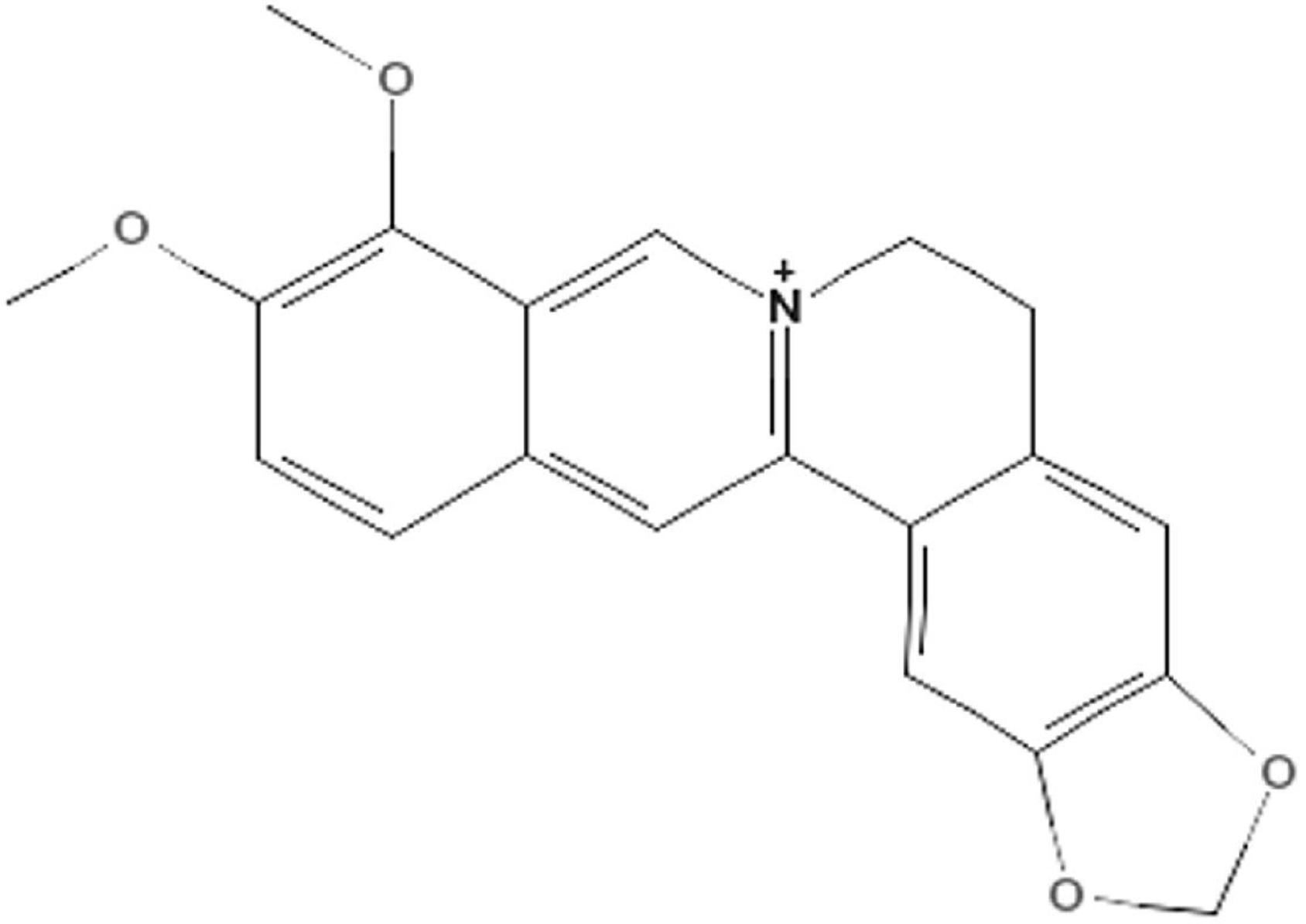

FIG.2

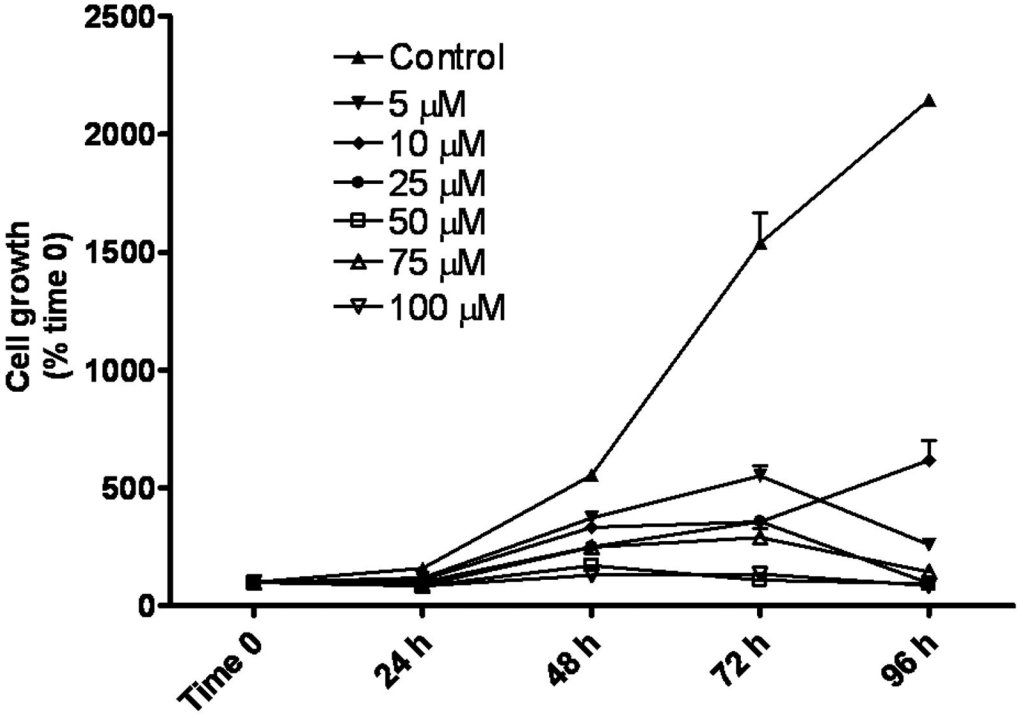
2500
2000
1500
1000
500
0
Cell growth
(% time 0)
Control
5 μM
10 μM
25 μM
50 μM
75 μM
100 μM
Time 0
24 h
48 h
72 h
96 h

FIG.3

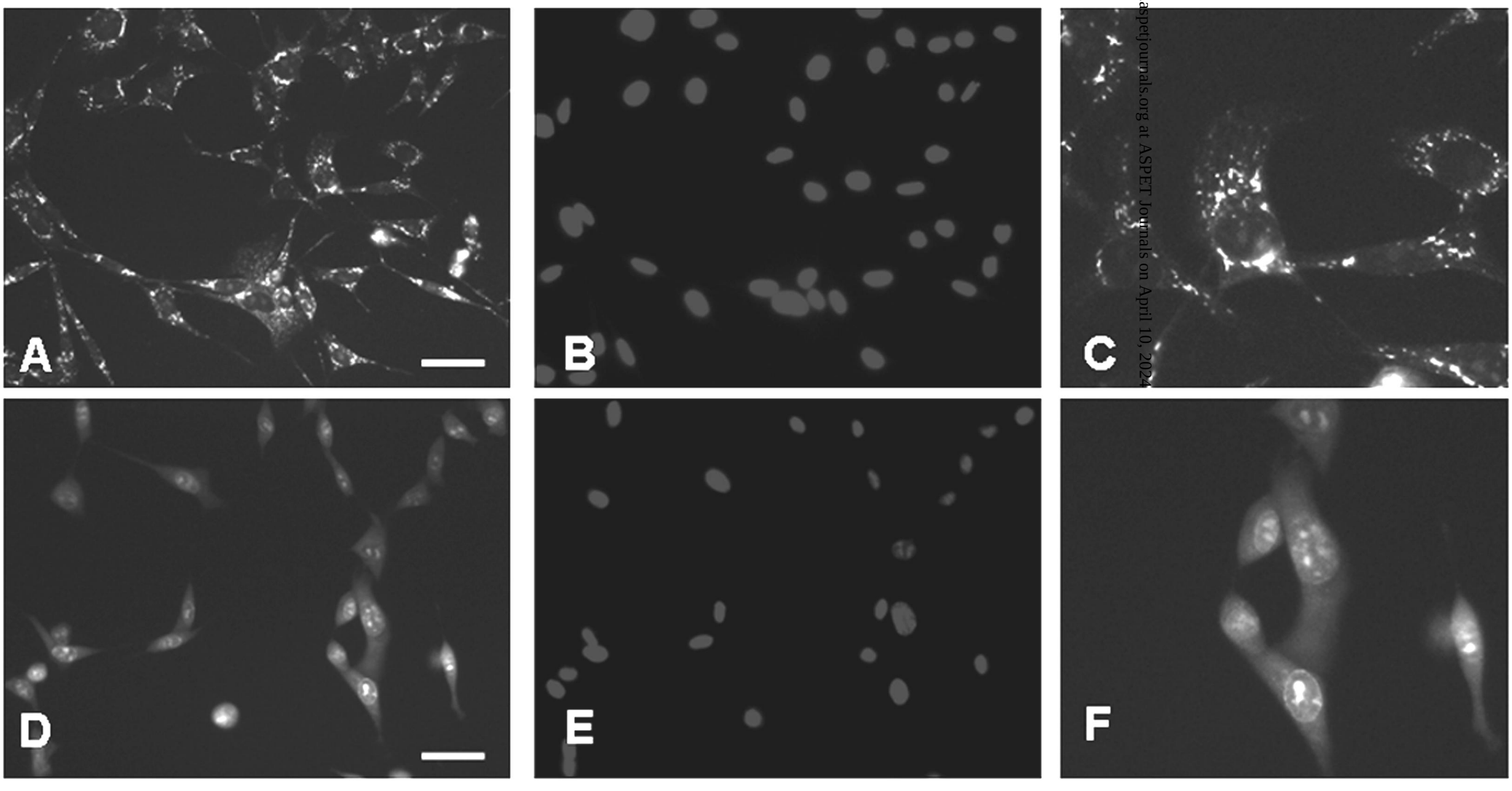

FIG.4

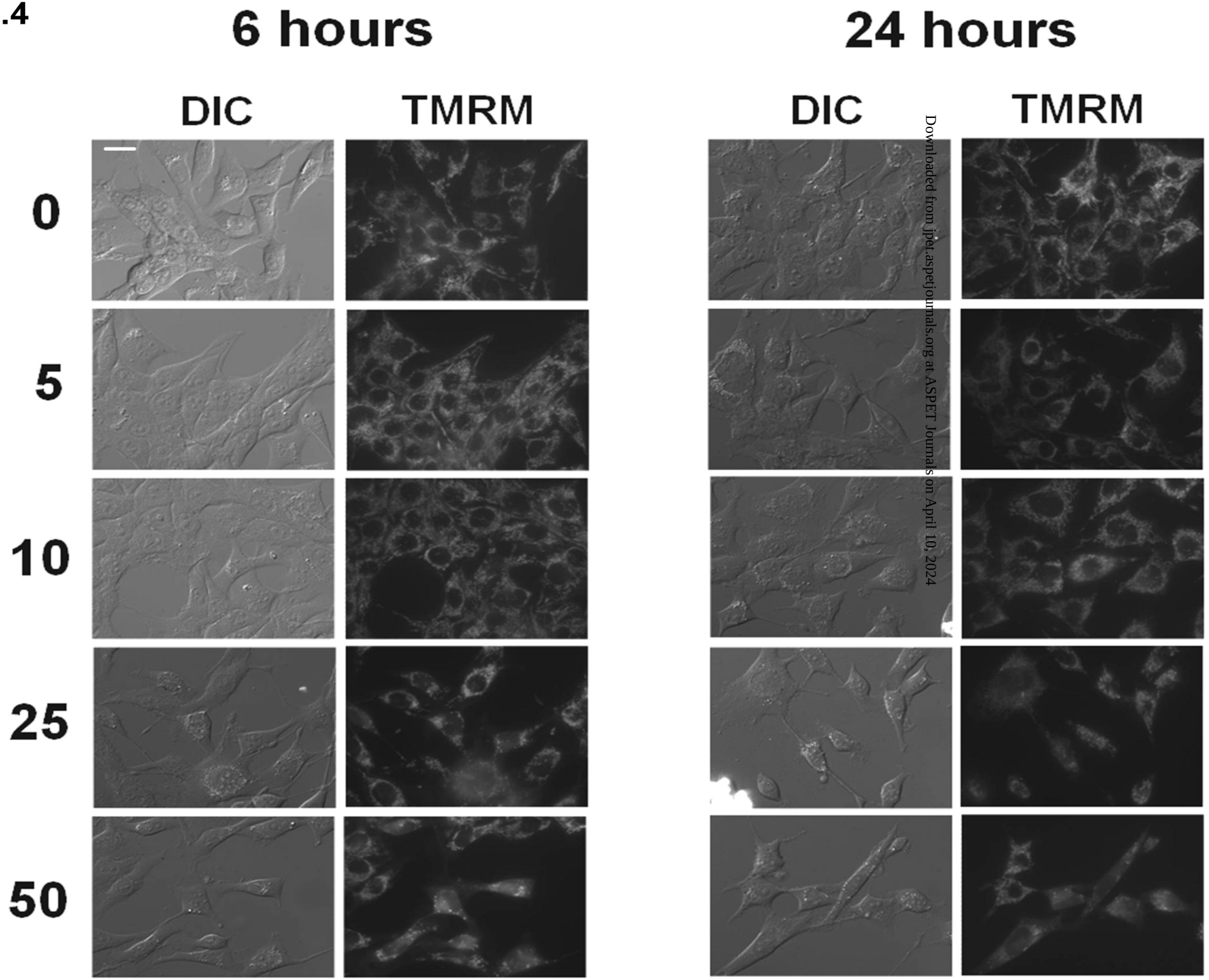

JPET Fast Forward. Published on August 17, 2007 as DOI: 10.1124/jpet.107.128017
This article has not been copyedited and formatted. The final version may differ from this version.

FIG.5

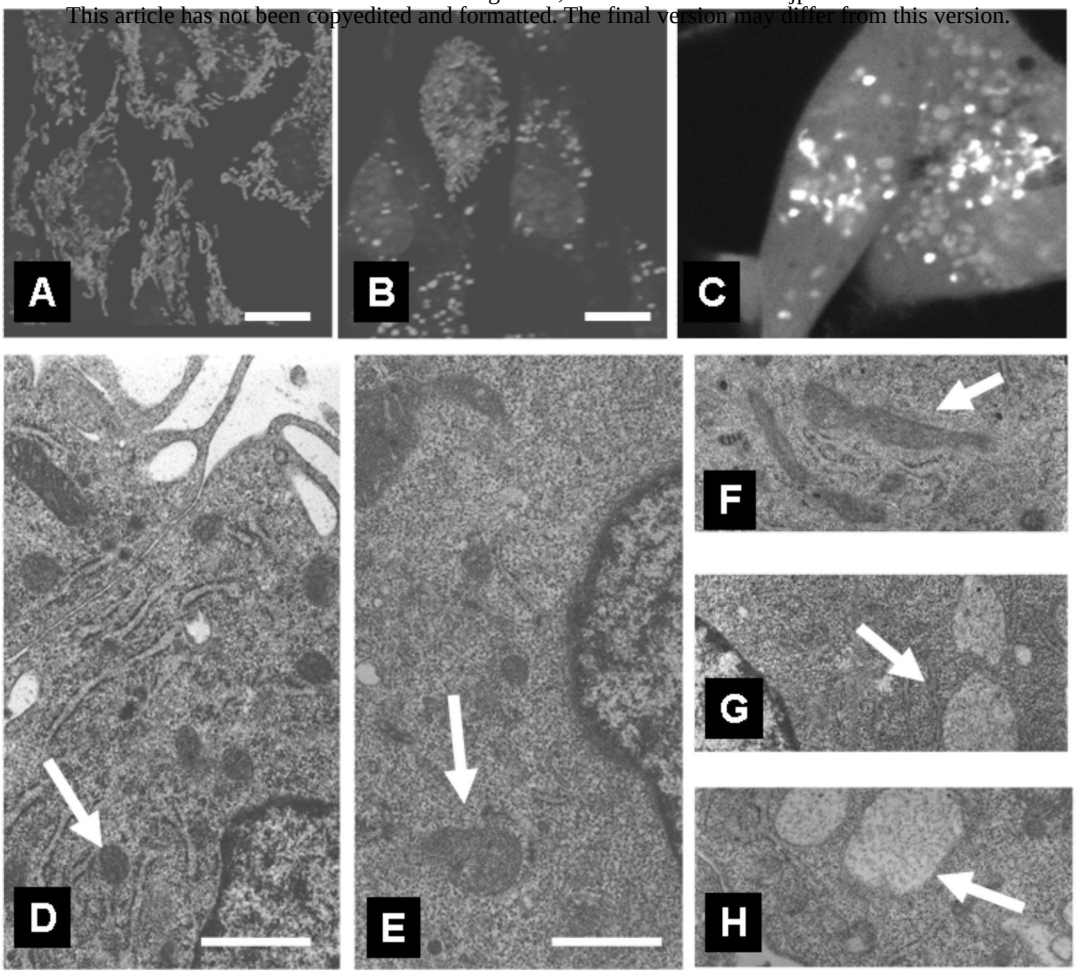

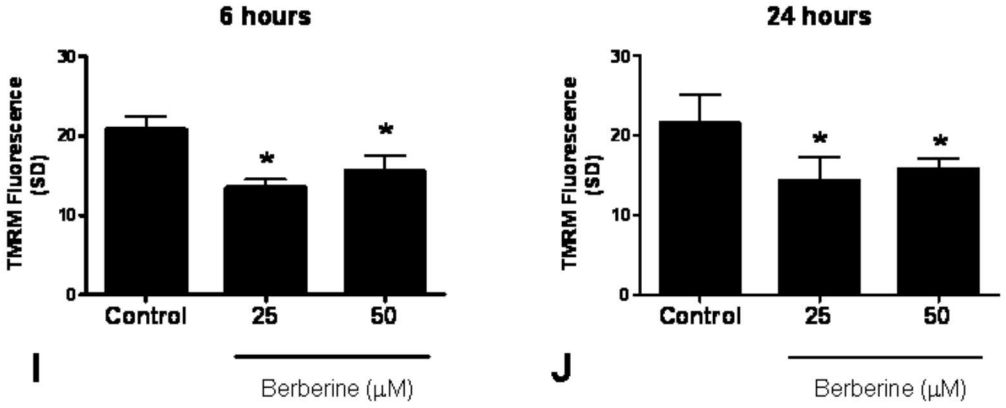

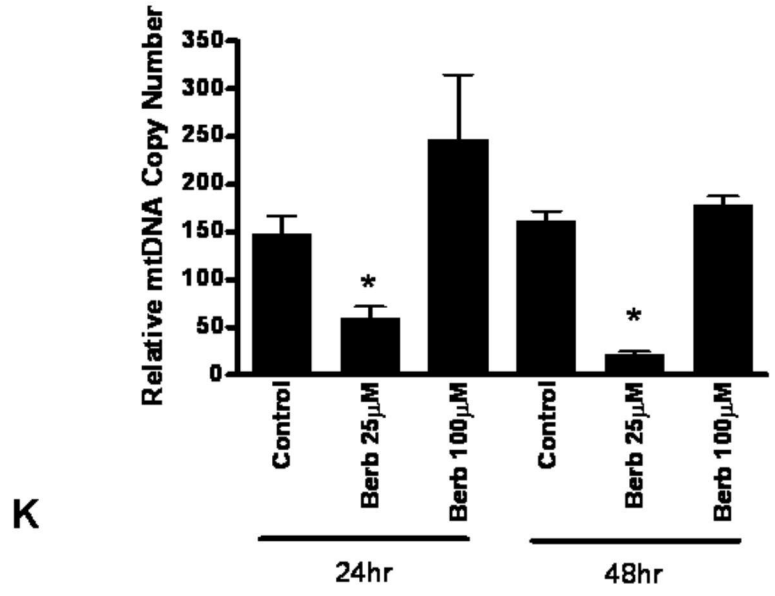

FIG.6

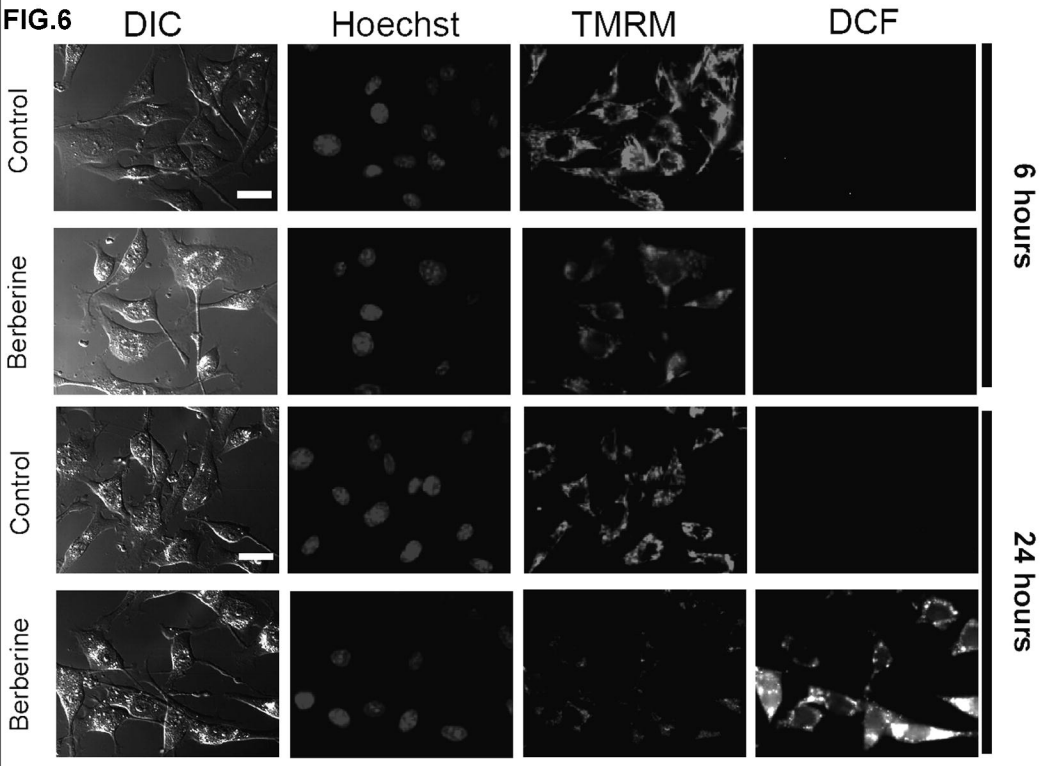
DIC
Hoechst
TMRM
DCF
Control
Berberine
Control
Berberine
6 hours
24 hours

FIG.7

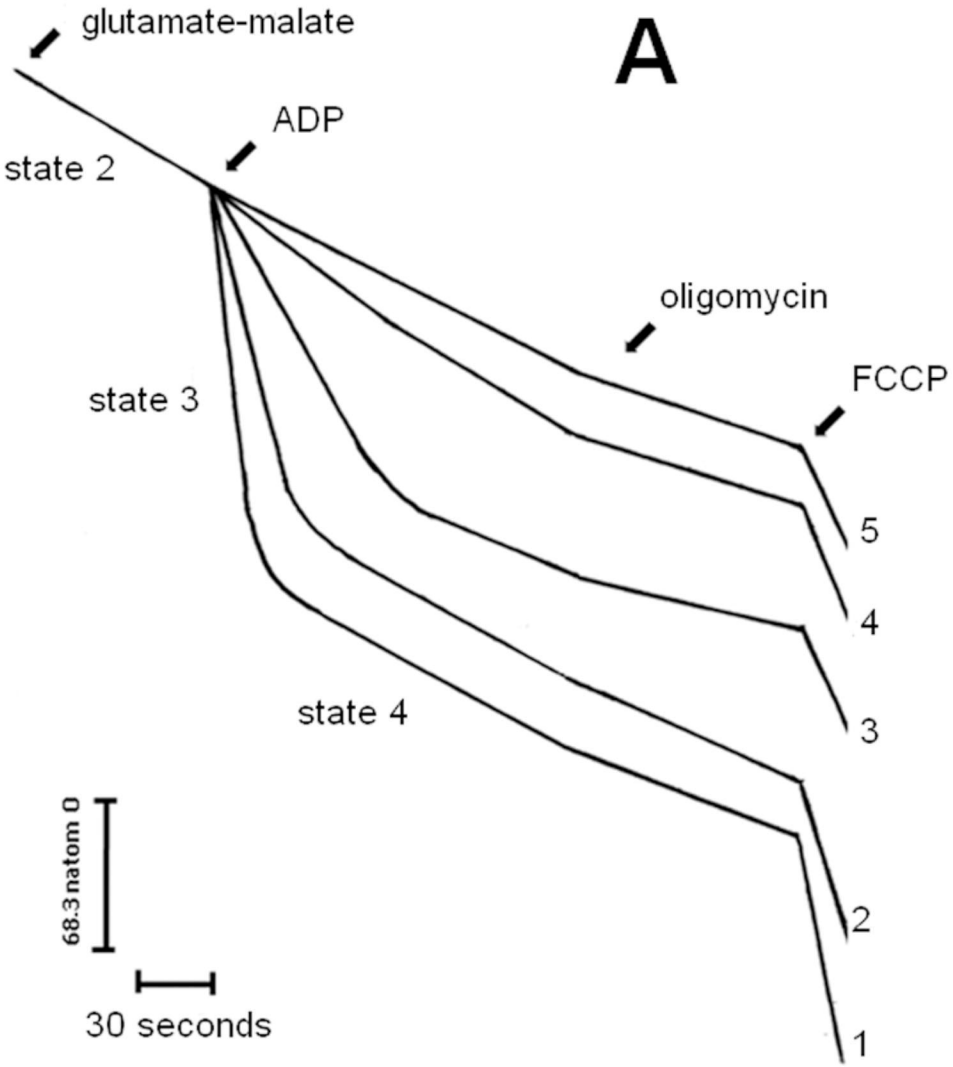

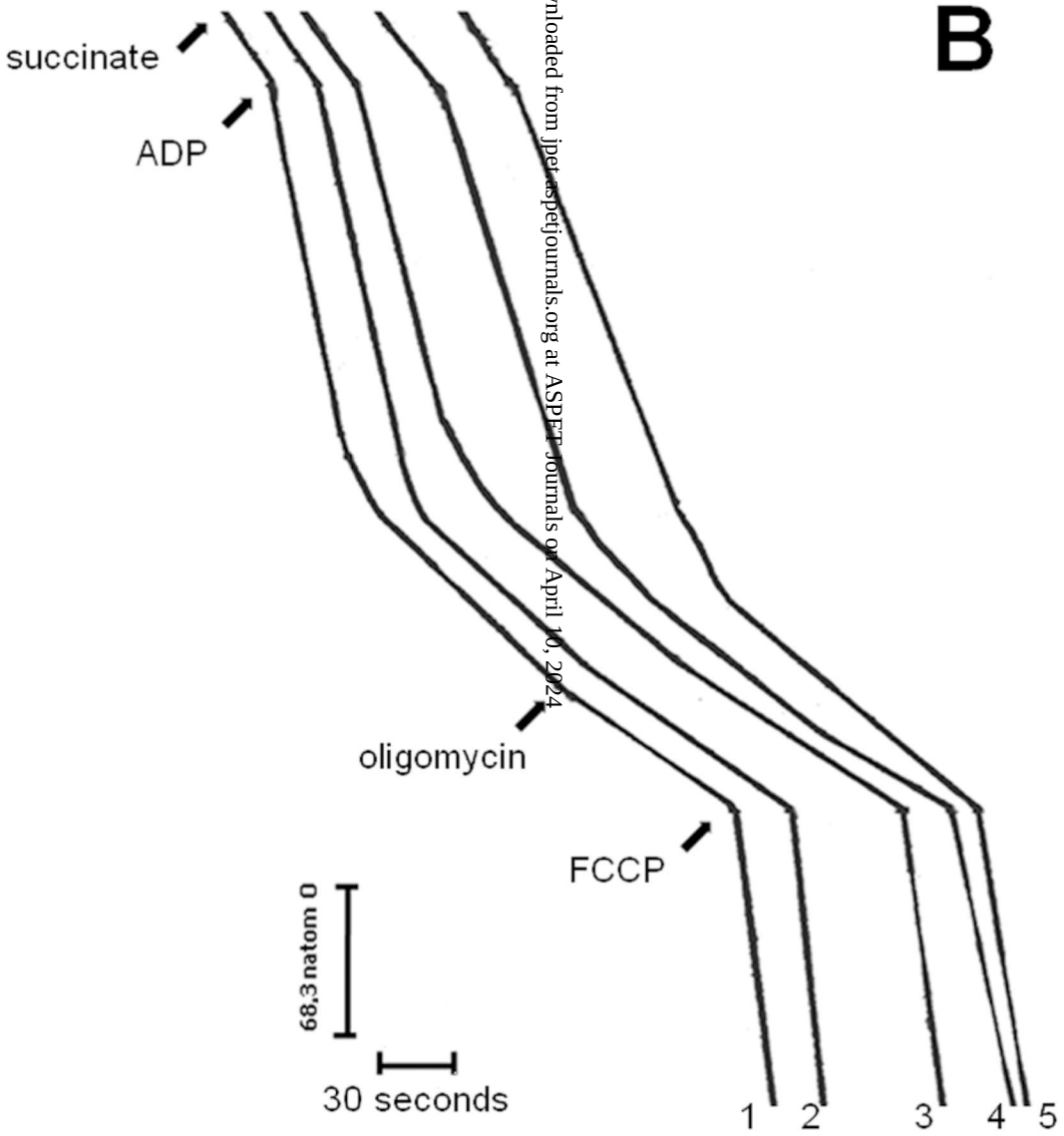

FIG.8

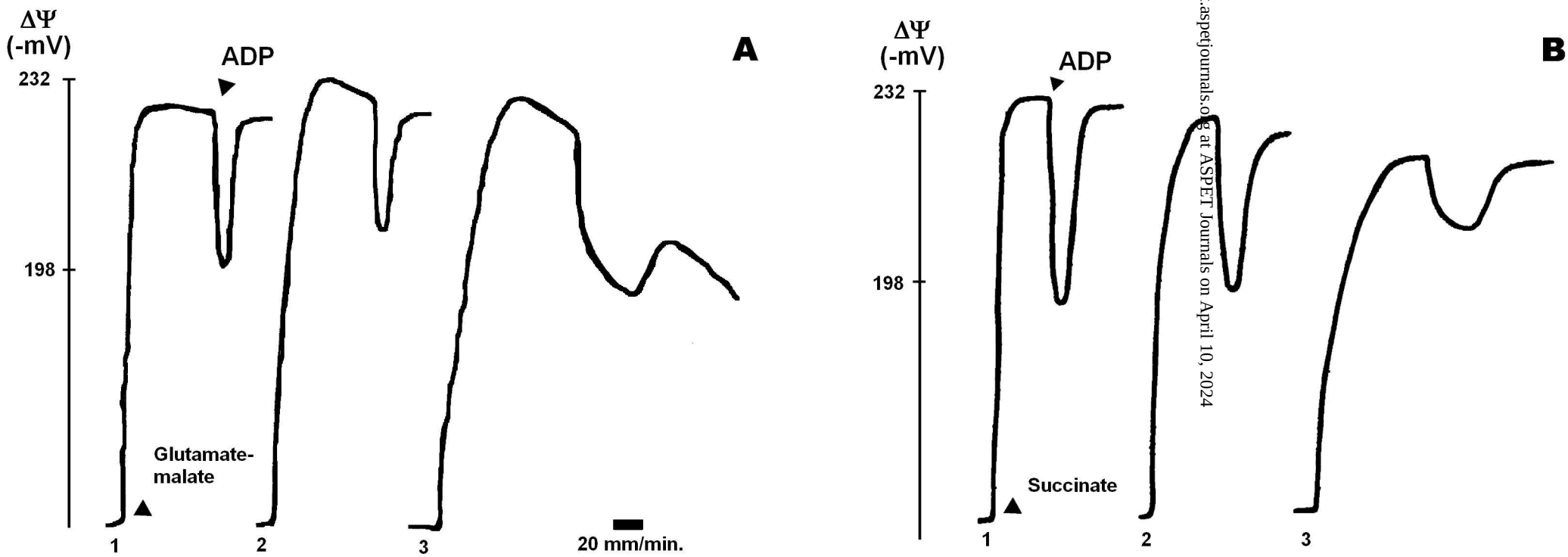

FIG.9

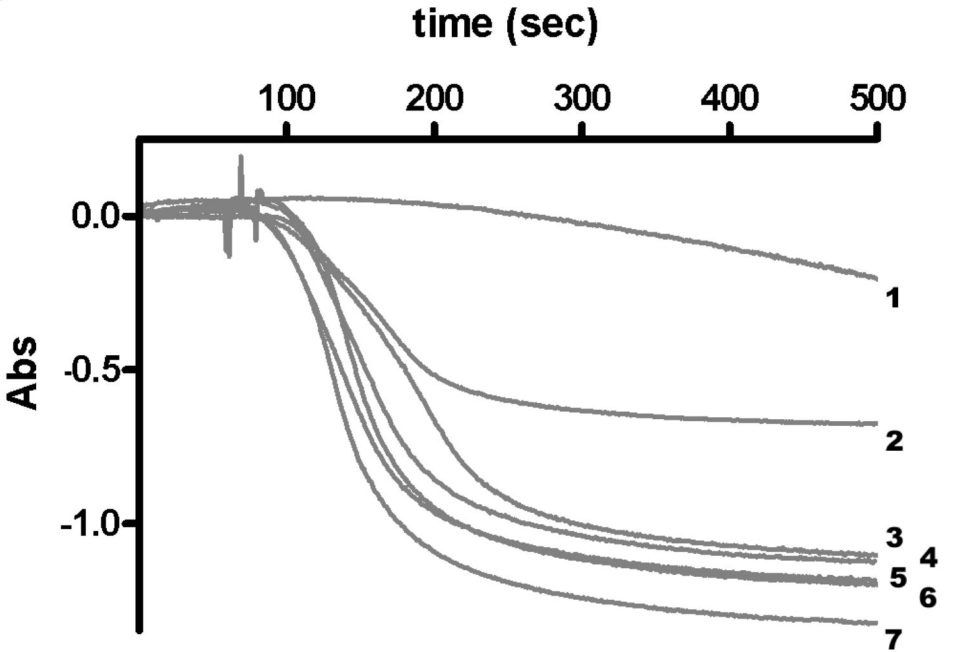

FIG.10

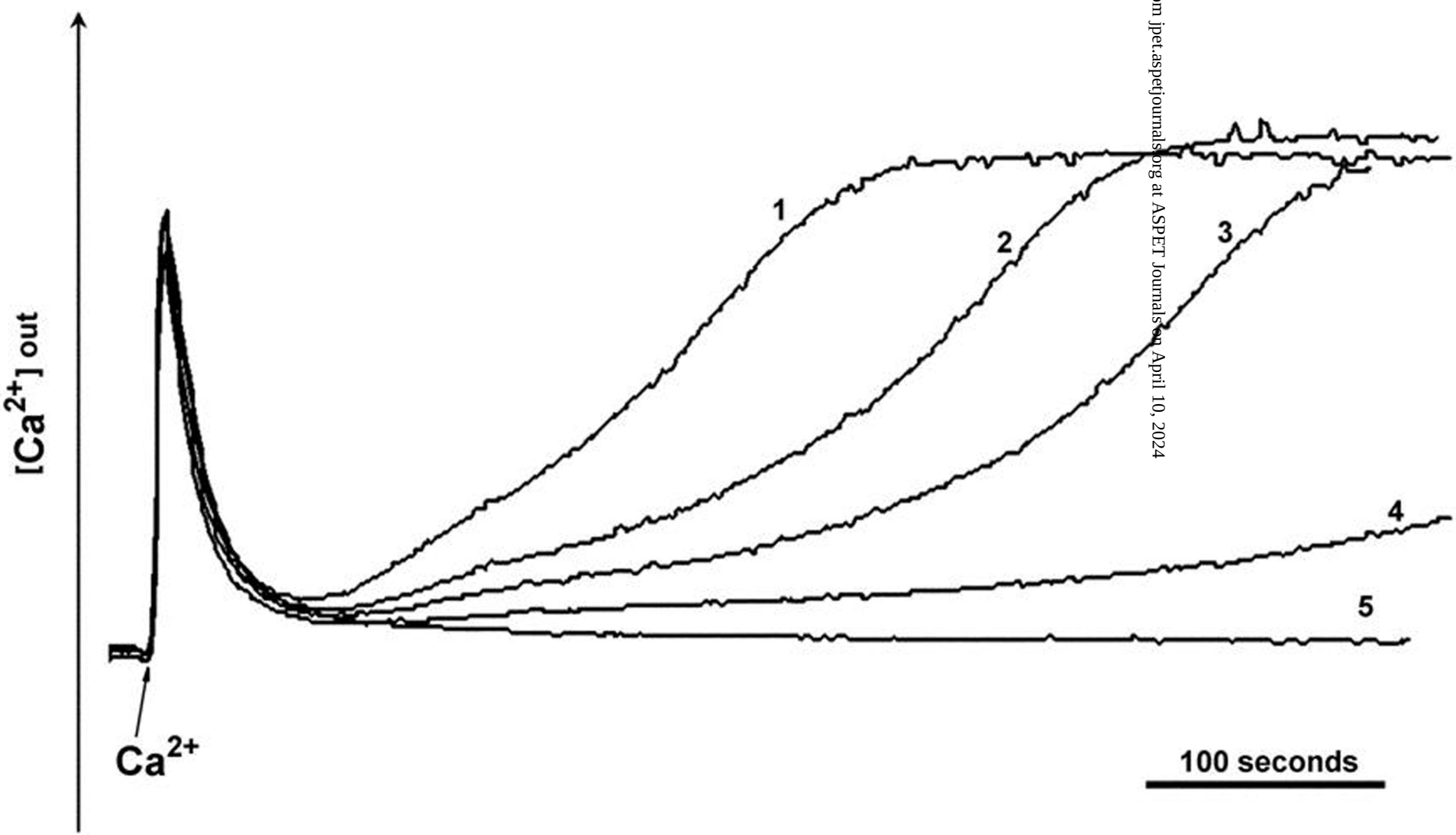

FIG.11

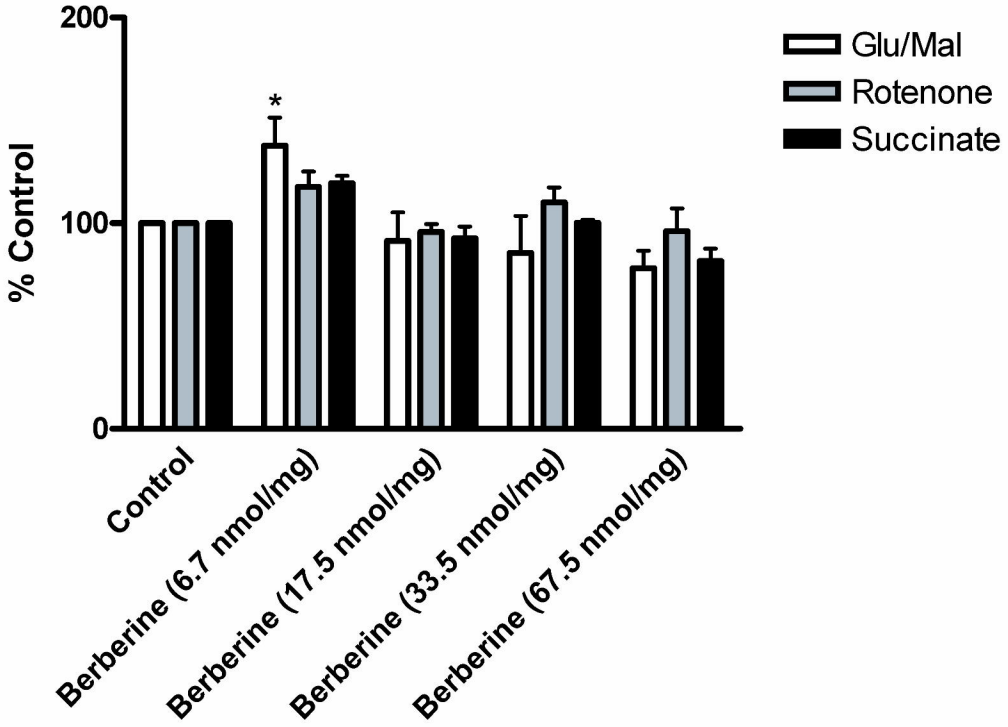
200
100
0
% Control
*
Glu/Mal
Rotenone
Succinate
Control
Berberine (6.7 nmol/mg)
Berberine (17.5 nmol/mg)
Berberine (33.5 nmol/mg)
Berberine (67.5 nmol/mg)